6-1999

Eta simulations of three extreme precipitation events: Sensitivity to resolution and convective parameterization

William A. Gallus Jr.
Iowa State University, wgallus@iastate.edu

Eta simulations of three extreme precipitation events: Sensitivity to resolution and convective parameterization

Abstract

A versatile workstation version of the NCEP Eta Model is used to simulate three excessive precipitation episodes in the central United States. These events all resulted in damaging flash flooding and include 16-17 June 1996 in the upper Midwest, 17 July 1996 in western Iowa, and 27 May 1997 in Texas. The episodes reflect a wide range of meteorological situations: (i) a warm core cyclone in June 1996 generated a meso-Î^{2}-scale region of excessive rainfall from echo training in its warm sector while producing excessive overrunning rainfall to the north of its warm front, (ii) a mesoscale convective complex in July 1996 produced excessive rainfall, and (iii) tornadic thunderstorms in May 1997 resulted in small-scale excessive rains. Model sensitivity to horizontal resolution is investigated using a range of horizontal resolutions comparable to those used in operational and quasi-operational forecasting models. Sensitivity tests are also performed using both the Betts-Miller-Janjic convective scheme (operational at NCEP in 1998) and the Kain-Fritsch scheme. Variations in predicted peak precipitation as resolution is refined are found to be highly case dependent, suggesting forecaster interpretation of increasingly higher resolution model quantitative precipitation forecast (QPF) information will not be straightforward. In addition, precipitation forecasts and QPF response to changing resolution are both found to vary significantly with choice of convective parameterization.

Keywords

floods, precipitation (meteorology), storms, thunderstorms, weather forecasting, convective parameterization, eta simulations, rain, flash flood, forecasting method, precipitation (climatology), weather forecasting, United States

Disciplines

Atmospheric Sciences | Geology | Meteorology

Comments

This article is from *Weather and Forecasting* 15 (1999): 405, doi: 10.1175/1520-0434(1999)014<0405:ESOTEP>2.0.CO;2. Posted with permission.

Eta Simulations of Three Extreme Precipitation Events: Sensitivity to Resolution and Convective Parameterization

WILLIAM A. GALLUS JR.

Department of Geological and Atmospheric Science, Iowa State University, Ames, Iowa

(Manuscript received 1 June 1998, in final form 15 January 1999)

ABSTRACT

A versatile workstation version of the NCEP Eta Model is used to simulate three excessive precipitation episodes in the central United States. These events all resulted in damaging flash flooding and include 16–17 June 1996 in the upper Midwest, 17 July 1996 in western Iowa, and 27 May 1997 in Texas. The episodes reflect a wide range of meteorological situations: (i) a warm core cyclone in June 1996 generated a meso-β-scale region of excessive rainfall from echo training in its warm sector while producing excessive overrunning rainfall to the north of its warm front, (ii) a mesoscale convective complex in July 1996 produced excessive rainfall, and (iii) tornadic thunderstorms in May 1997 resulted in small-scale excessive rains.

Model sensitivity to horizontal resolution is investigated using a range of horizontal resolutions comparable to those used in operational and quasi-operational forecasting models. Sensitivity tests are also performed using both the Betts–Miller–Janjic convective scheme (operational at NCEP in 1998) and the Kain–Fritsch scheme. Variations in predicted peak precipitation as resolution is refined are found to be highly case dependent, suggesting forecaster interpretation of increasingly higher resolution model quantitative precipitation forecast (QPF) information will not be straightforward. In addition, precipitation forecasts and QPF response to changing resolution are both found to vary significantly with choice of convective parameterization.

1. Introduction

As discussed in Doswell et al. (1996), flash flooding is currently the convective storm-related event producing the most fatalities annually in the United States. Several devastating flash floods in the 1970s (e.g., Rapid City, SD; Big Thompson Canyon, CO; Johnstown, PA) resulted in a needed research emphasis aimed at improved flash flood prediction (e.g., Hoxit et al. 1978; Maddox et al. 1978). The result of this emphasis has been a better understanding of the synoptic settings associated with excessive rainfall events (Maddox et al. 1979). Although many lives have undoubtedly been saved with the improvements in forecasting of these events, flash flood forecasting remains a difficult challenge, and the number of annual fatalities remains high relative to tornadoes or hurricanes.

Short-term forecasting (under 6–12 h) of flash floods relies heavily upon radar data depicting ongoing convection. Longer-term forecasting (generally 12–48 h) has been difficult, at least partly because maximum quantitative precipitation forecasts (QPFs) are somewhat constrained by the horizontal resolution of numerical models. Junker and Hoke (1990) found that convective rain amounts were underestimated in general by a factor of 2 or more by numerical models at that time. A study of excessive rain events in the Mediterranean region also found that peak precipitation was underestimated, even though simulations were performed with a mesoscale model having 20-km horizontal resolution (Romero et al. 1998). Operational forecasters traditionally have had to somewhat arbitrarily magnify model-predicted rainfalls in potential excessive rainfall events and make judgments about model-predicted locations of the peak precipitation.

The use of increasingly fine horizontal resolution in operational numerical weather prediction models (e.g., Black 1994; Rogers et al. 1998) has generally improved quantitative precipitation forecasting, at least as indicated by traditional skill scores (Mesinger 1998). Increased horizontal resolution allows greater vertical motions to be resolved in a model (Weisman et al. 1997), with a corresponding increase in moisture transport that would likely result in increases in the peak predicted precipitation. It is possible that improvements in simulated precipitation amount would be most pronounced for extreme precipitation events (e.g., Nicolini et al. 1993), which would tend to occur in regions of abundant moisture and strong ascent.

Corresponding author address: Dr. William A. Gallus Jr., Department of Geological and Atmospheric Science, Iowa State University, 3025 Agronomy Hall, Ames, IA 50011.
E-mail: wgallus@iastate.edu

From a hydrological perspective, the forecasting of flash flooding resulting from excessive rainfall not only depends on accurate forecasts of precipitation but also on the size and orientation of the drainage basins involved (Senesi et al. 1996). For river stage forecasting over large basins, current errors in model QPFs may result in limited errors in the stage forecasts, since a simulated region of excessive precipitation can have a large position error and still lie within the basin. In addition, for a large basin, the average precipitation over a sizable region will be of more importance than the peak precipitation at one model grid point. However, for increasingly small basins, the use of mesoscale model QPFs can result in increasingly large errors in flood forecasts. At least partly motivated by this risk, ensemble approaches are being investigated for precipitation forecasts (Du et al. 1997; Hamill and Colucci 1998). Short-range ensemble forecasts of precipitation have shown some increased skill in comparison to a single higher-resolution forecast; however, the tendency for ensemble averaging to result in smoothing may be detrimental to some precipitation forecasts for extreme events. In addition, the ensemble approach is still somewhat limited by the accuracy of the model and analysis systems used (Du et al. 1997).

As improvements in horizontal resolution continue to be made, forecasting of excessive precipitation will be affected. In theory, simulated heavy amounts of precipitation in excessive rainfall events should begin to approach the large amounts observed. If so, fundamental changes will be necessary for operational forecasters who may no longer need to adjust model-predicted amounts to determine maximum precipitation potential for cases with a flash flood risk. However, as long as horizontal resolutions remain sufficiently coarse as to require the use of convective parameterizations, the changing behavior of these parameterizations as resolution improves may complicate interpretation (e.g., Molinari and Dudek 1986; Zhang and Fritsch 1988; Molinari and Dudek 1992). Zhang et al. (1994) have also found that the treatment of interaction between subgrid-scale and grid-resolvable precipitation significantly impacts simulations. Hong and Pan (1998) note that the location of the grid-resolved precipitation is more influenced by the convective parameterization than by changes in the grid-resolvable precipitation algorithm itself. In addition, the timing of activation of both the convective parameterization and the explicit moisture scheme has been found to have an extremely significant impact on simulations (Grell 1993) and can vary markedly with different parameterizations.

To gain insight into the effect that horizontal resolution has on predicted rainfall for extreme events, a series of simulations has been performed using a workstation version of the National Centers for Environmental Prediction's (NCEP) Eta Model. A detailed description of the Eta Model and some of the more recent modifications can be found in Mesinger et al. (1988), Janjic (1994), Black (1994), Chen et al. (1996), and Rogers et al. (1998). The workstation version of the model shares the same dynamic code and physical parameterizations as the operational version (as of late 1997) but allows significant flexibility in choice of domain, resolution, and initial and boundary condition data.

Because excessive rainfall can occur from a variety of meteorological conditions (e.g., Doswell et al. 1996), three cases have been chosen to be investigated with the model. The precipitation associated with each event can be seen in Fig. 1. The first case to be examined occurred on 16–17 June 1996 in the upper Midwest (Fig. 1a). A warm core synoptic-scale cyclone traveled northeastward, resulting in the training of convective echoes during the late afternoon and early evening hours in a meso-β-scale region within the warm sector near central Iowa (along with extensive excessive rainfall later, primarily after 1200 UTC 17 June, in Wisconsin in an overrunning region north of the warm front). In the second case (Fig. 1b), a mesoscale convective system (MCS) developed in northeastern Nebraska late on 16 July 1996 and traveled east-southeastward during the night into Iowa on 17 July, producing a small-scale area of excessive rains. Finally, a case will be examined from 27 May 1997 when intense tornadic thunderstorms traveled in a strongly deviant motion from the mean flow across central and southern Texas (Fig. 1c). Small-scale areas experienced excessive rainfall and flash flooding during the afternoon and evening with this event, which was apparently initiated or influenced by a southwestward propagating gravity wave produced by earlier convection (Corfidi 1998).

Because convective precipitation was important in all three cases, and the appropriateness and behavior of different convective parameterizations is known to vary with changing horizontal resolution, two different convective schemes were used in the simulations to be discussed. The Betts–Miller–Janjic (BMJ hereafter) scheme (Betts 1986; Betts and Miller 1986; Janjic 1994) has traditionally been used in the Eta Model and was operational in 1998. The Kain–Fritsch (KF hereafter) convective parameterization (Kain and Fritsch 1992; Kain and Fritsch 1993) was developed specifically for use in models with mesoscale resolution. Numerous studies have demonstrated the impact that differences in the design of convective parameterizations can have on simulated convection (e.g., Grell 1993; Rogers and Fritsch 1996). It is not the purpose of this paper to judge one scheme as inherently better or worse than the other. Instead, the two schemes were chosen to demonstrate the variability in model forecasts, both due to differing horizontal resolution and differing precipitation physics, that will likely continue to confront forecasters in the coming years, and to reveal the complexity of the QPF challenge.

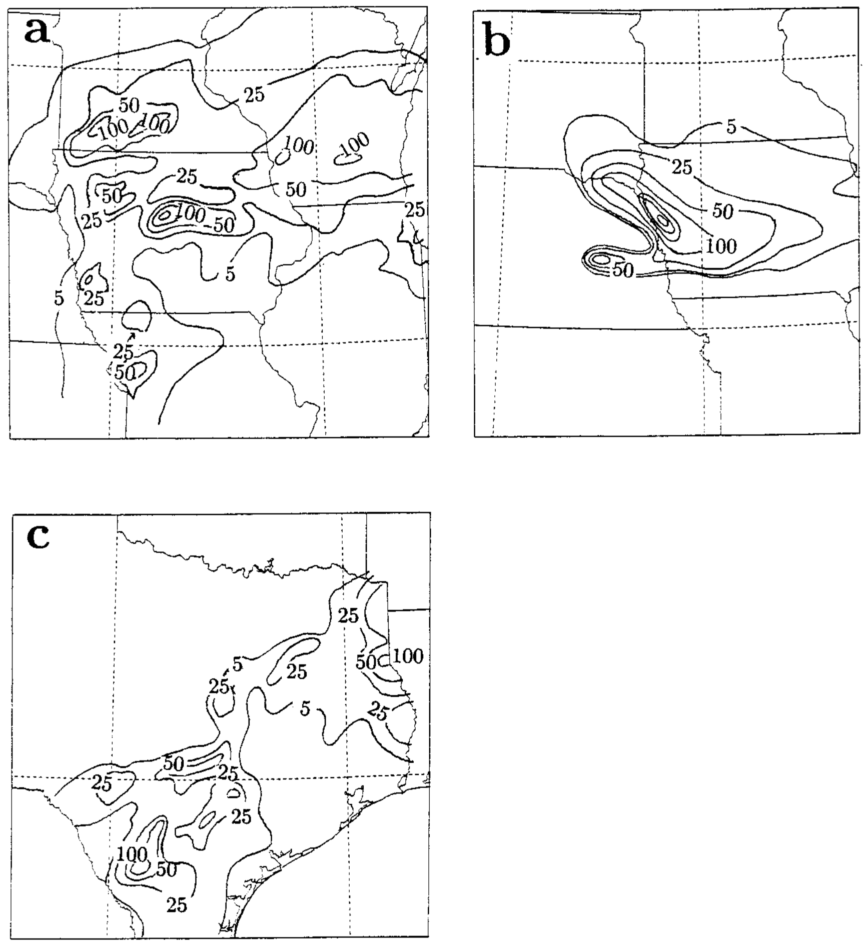

FIG. 1. Observed rainfall (mm) for three flash flood events: (a) 1200 16 Jun–1200 UTC 17 Jun 1996, (b) 1200–1200 UTC 16–17 Jul 1996, and (c) 1200–0600 UTC 27 May 1997. Contours are shown for 25, 50, 100, 150, 200, and 300 mm.

2. Observational analyses

a. 16–17 June 1996

Damaging flash flooding and record river flooding occurred in a small part of central Iowa around the city of Ames on 16–17 June 1996 after 150–225 mm of rain fell in a 4–6-h period centered on the late afternoon and early evening hours. The accumulated rainfall, determined from cooperative observer reports in the publication *Climatological Data,* during the 24-h period from 1200 UTC 16 June through 1200 UTC 17 June can be seen in Fig. 1a. A larger area of excessive rainfall would occur in the following 24 h across much of Wisconsin (with storm totals exceeding 325 mm), resulting in additional record flooding.

Large-scale parameters were favorable for excessive rainfall over much of the upper Midwest in this event as a subtropical warm core cyclone moved northeastward toward the region. Flash flood watches had been issued for various areas well in advance of the excessive rainfall. A sounding from Topeka, Kansas (in the warm sector of the low, upstream from central Iowa), at 1200 UTC 16 June (Fig. 2) shows the high values of low-level moisture present, along with exceptionally warm temperatures aloft (−5°C at 500 mb). In spite of the midlevel warmth, convective inhibition (CIN) was relatively small with an attainable convective temperature of 29°–30°C and a significant amount of convective available potential energy (CAPE), 1500 J kg^{-1}, when using average potential temperature and mixing ratio values in the lowest 500-m layer. Dewpoint temperatures at 850 mb and 700 mb were around 18° and 8°C, respectively, with both of these values exceeding the averages found for all flash flood classifications defined by Maddox et el. (1979). The precipitable water here, and in a sizable region moving into Iowa from the southwest, was around 50 mm.

An MCS had developed and moved across western Iowa prior to 1200 UTC 16 June, dropping 25–50 mm of rain along a north–south axis just west of the center of the state. During the morning hours, this MCS dissipated as it moved into eastern Iowa. By 1800 UTC,

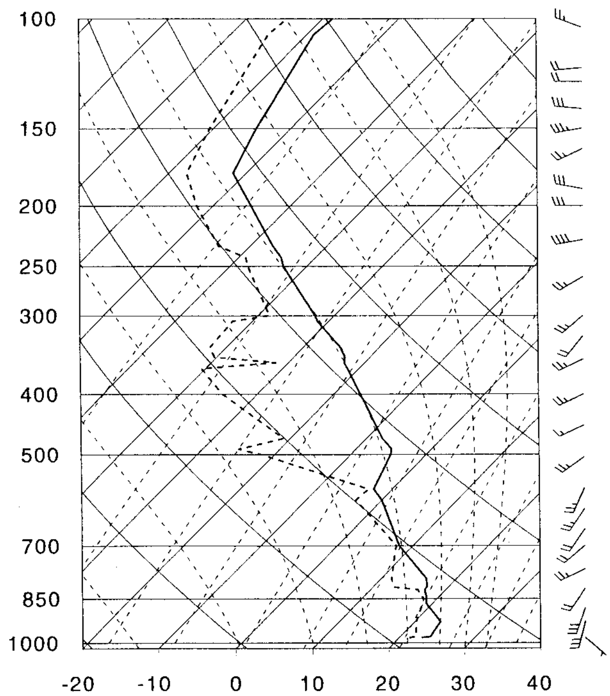

FIG. 2. Skew *T*–log*p* diagram from Topeka, KS, at 1200 UTC 16 Jun 1996. Temperature (solid) and dewpoint (dashed) are plotted.

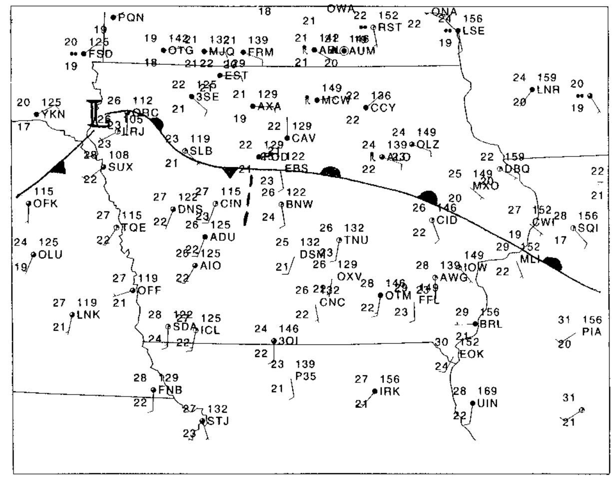

FIG. 3. Surface map at 1800 UTC 16 Jun. Conventional notation is used for fronts. Dashed line in central Iowa indicates region of confluence along a possible outflow boundary. Station plot includes temperature (upper left) and dewpoint (lower left) in °C, altimeter setting (tenths of mb, leading 10 dropped), and winds (m s^{-1}; full barb is 5 m s^{-1}).

skies had partially cleared over much of Iowa south of the warm front (Fig. 3), and surface dewpoints had risen to between 21° and 24°C over much of this region. A surface low-pressure system was moving eastward into the western part of the state at this time. North of the warm front, an extensive area of rain and embedded thunderstorms continued. A weak convective boundary may have been present near the central part of the state, inferred from the south-southeasterly winds at Boone (BNW) and Webster City (EBS) compared with general southwesterly winds over much of the rest of western Iowa. The thermal contrast along this boundary was negligible; a study of tornadic thunderstorms has indicated that the spindown time for horizontal vorticity decay is at least several hours, and boundaries can thus lose their thermal contrast while still being identifiable as regions of horizontal wind shear (Markowski et al. 1998a,b).

This boundary persisted for the next several hours and can be seen slightly enhancing the moisture convergence field along a north–south line in central Iowa at 2100 UTC (dashed line in Fig. 4). The strongest moisture convergence was occurring along the warm front in northern Iowa (where some tornadic thunderstorms were developing) and along the surface trough in far eastern Nebraska. A fairly significant area of new convection had developed between 2000 and 2100 UTC in western Iowa, showing up as a small region of moisture divergence, with a narrow line of isolated thunderstorms initiating around 2100 UTC on a southwest–northeast axis from about Audubon (ADU) to just northeast of BNW (see Fig. 3 for site locations).

Over the next few hours, the larger and more intense region of convection in western Iowa moved eastward and weakened, while cells along the convergence line near Boone intensified dramatically. The cloud shields associated with the two regions of convection merged by 0000 UTC, and at this time rainfall rates of 50–75 mm h^{-1} were occurring in parts of central Iowa. Some unofficial reports mentioned over 160 mm of rain in 2 h in this area. The intensity of the convection in central Iowa caused a distinct mesolow to form near BNW with an outflow boundary nearby extending some distance

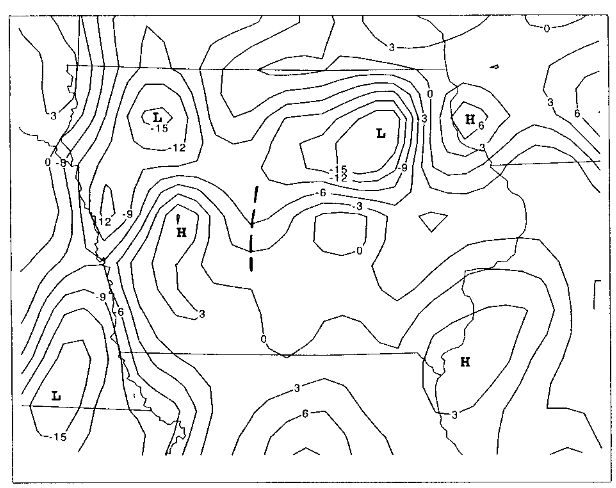

FIG. 4. Moisture divergence ($\times 10^{-4}$ g kg^{-1} s^{-1}) at 2100 UTC 16 Jun. Contour interval is 3×10^{-4} g kg^{-1} s^{-1}, with negative values indicating convergence. Area of enhancement in region of later excessive rainfall indicated with a dashed line.

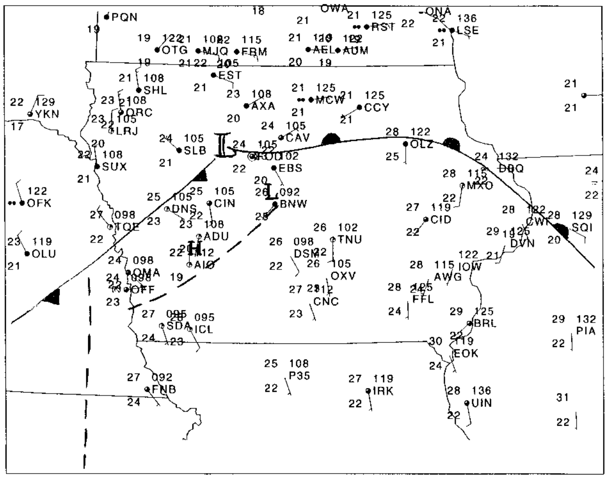

FIG. 5. As in Fig. 3 except at 0000 UTC 17 Jun.

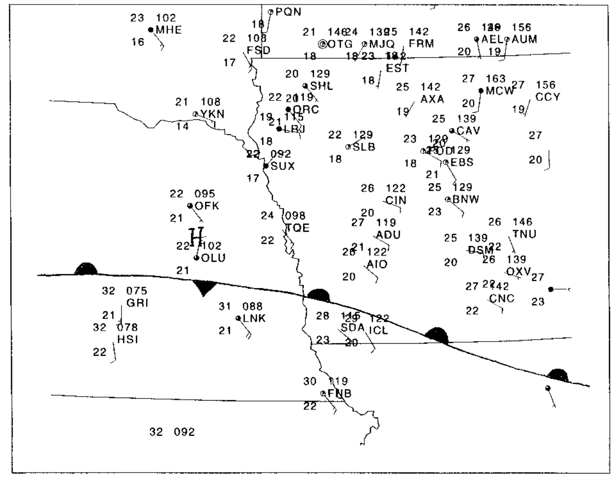

FIG. 6. Surface map at 0000 UTC 17 Jul 1996. Notation as in Fig. 3.

to the southwest at 0000 UTC (Fig. 5). Flow continued to back ahead of the system, with southeasterly wind supplying significant low-level moisture. Surface dewpoints over a wide region on the inflow side of the thunderstorms were between 22° and 24°C. High reflectivity echoes would continue to propagate northeastward along the outflow boundary until around 0300 UTC, at which time the system finally developed a more southeastward component of propagation.

The excessive rainfall that occurred in central Iowa was generally confined to a 4–6-h period (~2200–0300 UTC), with the heaviest amounts (150–225 mm) confined to an area of only around 500 km^2. However, the rainfall was centered over the basins of two waterways that flow south into the city of Ames. The resulting floods established a new record crest on one of the waterways and a third highest crest of record on the other. Extensive damage resulted.

North of the warm front, heavy rains would continue to fall throughout 17 June, with some locations in Wisconsin receiving over 325 mm of rain in a 36-h period. The excessive rains in this region covered a larger area, and several record river crests occurred in the following days.

b. 16–17 July 1996

During the night of 16–17 July 1996, an MCS developed in extreme northeastern Nebraska and traveled east-southeastward in a fairly common fashion into Iowa. Numerous reports of hail and tornadoes occurred during the development of the system in eastern Nebraska around 0000 UTC 17 June, followed by up to 300 mm of rain in portions of western Iowa (Fig. 1b). Severe flash flooding and some record river crests were experienced in northeastern Nebraska and western Iowa. Compared to the 16–17 June 1996 event, the area of excessive rainfall (generally greater than 100 mm) generated by the convection was significantly larger, and the MCS itself occurred on a larger scale.

The large-scale weather pattern during this event was typical of that associated with MCS/Mesoscale Convective Complex (MCC) activity. At the surface at 0000 UTC (Fig. 6), a slow-moving warm front extended east–west across southern Nebraska and southern Iowa, with a large temperature contrast (~10°C) across it. Thunderstorms had already formed by this time in portions of east-central and northeastern Nebraska, north of the front where isentropic lift was strong. Although the Omaha sounding at 0000 UTC 17 July was taken north of the surface front, significant low-level moisture can be seen in the sounding (Fig. 7) with an 850-mb dewpoint of ~17°C. Flow from the surface upward through 800 mb had a strong southerly component at around 10 m s^{-1}, favoring lift over the front. During the night, the low-level flow intensified as the low-level jet reached speeds of 15–20 m s^{-1} (figure not shown). Precipitable water in much of southeastern Nebraska was between 45 and 48 mm. Although CIN for the lowest 500-m layer in the sounding was around 100 J kg^{-1}, CIN for air parcels just above the inversion was less than 25 J kg^{-1} with CAPE exceeding 2000 J kg^{-1}.

The developing convection at 0000 UTC later organized into an MCS dropping excessive rainfall in western Iowa by 0600 UTC. Winds below 250 mb in the sounding were not particularly strong, generally below 15 m s^{-1}, so that rapid storm motion would not be expected from the mean wind vector. The 850–300-mb thermal wind indicated a southeastward movement for any MCS that would develop. The Corfidi vector approach (Corfidi et al. 1996), taking into account the predicted low-level jet (~17.5 m s^{-1} from 200° at 0600 UTC) from the operational Eta Model initialized at 0000 UTC, suggested movement of the most intense meso-β elements toward the south-southeast at 10–15 m s^{-1}, not a particularly slow speed.

The convective system had weakened by 1200 UTC

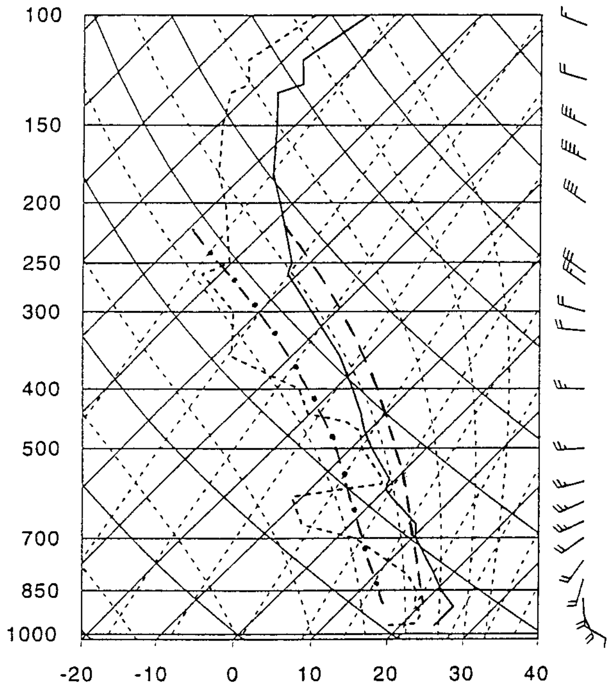

FIG. 7. As in Fig. 2 but for Omaha, NE, at 0000 UTC 17 Jul 1996. Examples of reference temperature and dewpoint curves as used in the BMJ scheme are shown with long-dashed and dashed–dotted curves, respectively.

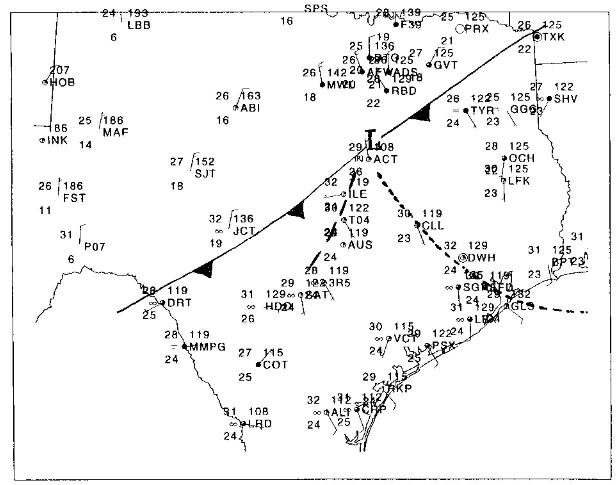

FIG. 8. As in Fig. 3 except for 1800 UTC 27 May 1997. Location of gravity wave (inferred from satellite data) indicated with short-dashed line.

as it moved into portions of central Iowa. In general, the most intense convective elements during the night had moved east or southeast at 10–15 m s^{-1}, with redevelopment on the southwest sides of the cells, resulting in echo training in the region experiencing 100–300 mm of precipitation. Less intense rainfall did spread east-southeastward across much of Iowa. Interestingly, the general large-scale weather pattern would remain basically unchanged through the following 24 h, and a state record for 24-h precipitation was set later on 17–18 July in northern Illinois as repeated MCS activity dropped over 400 mm of rainfall there.

c. 27 May 1997

Despite marginally strong winds at most levels, a significant tornado outbreak occurred in central Texas on 27 May 1997, apparently facilitated by the interaction of several mesoscale boundaries. The mesoscale influences included a southwestward propagating gravity wave (evidenced by alternating thickening and thinning of capped mixed layer cloudiness as seen in satellite imagery) generated from early morning convection in Arkansas (Corfidi 1998). The gravity wave intersected a slow-moving cold front, releasing extreme conditional instability. Afternoon surface temperatures exceeding 30°C were accompanied by dewpoint temperatures as high as 26°C along the front. In addition to several significant tornadoes, the convection produced local rainfalls exceeding 100 mm (Fig. 1c), primarily during the afternoon and early evening hours, with at least one fatality attributed to flash flooding.

The most significant convection during this event began around 1800 UTC near Waco, Texas (ACT). At the surface at this time (Fig. 8) a slow-moving cold front was located from near Junction, Texas (JCT), to Texarkana, Arkansas (TXK). A mesoscale area of lower pressure was present near Waco. Strong sustained moisture convergence that had been occurring since sunrise near the front had helped maintain extremely high surface dewpoints in the region. A west wind at Killeen (ILE) may have been evidence of a boundary ahead of the front. A gravity wave propagating southwestward was approaching Waco at this time (shown with dotted line; position determined from satellite imagery) and appeared to enhance developing convection near there.

No soundings were available from the region of central Texas where convection would later be most intense, and the nearest sites at 1200 UTC were unrepresentative of conditions where the convection occurred. (The nearest soundings at 1200 UTC indicated a strong capping temperature inversion above a shallow 50–100-mb layer of moisture near the surface). A modified sounding valid at 1800 UTC for the region near Jarrell in central Texas is shown in Fig. 9. Thermodynamic data shown in the figure are based on a National Oceanic and Atmospheric Administration (NOAA) *Geostationary Operational Environmental Satellite-8* (*GOES-8*) sounder-derived thermodynamic profile (D. Gray 1998, personal communication) modified somewhat using 0000 UTC 28 May conditions at Del Rio (DRT) and Corpus Christi (CRP), Texas (locations shown in Fig. 8), with winds taken from the Eta forecast valid at 1800 UTC. The *GOES-8* profile used the 1200 UTC 27 May operational Eta Model 6-h forecast as a ''first guess'' for the temperature and moisture values, with adjustments made

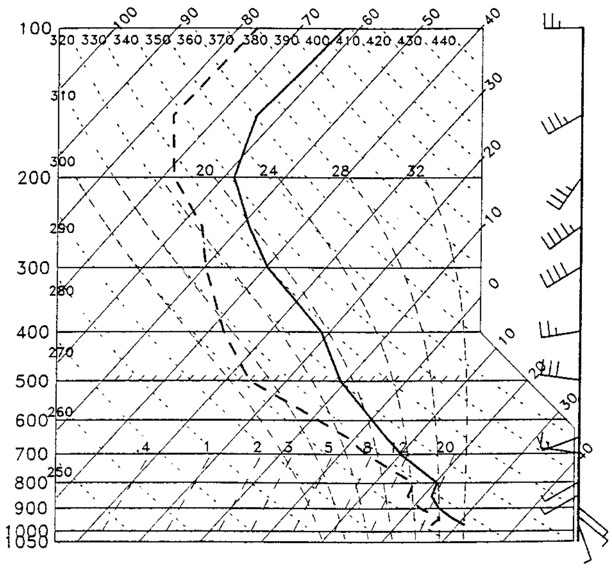

FIG. 9. As in Fig. 2 but for estimated conditions near Jarrell in central Texas at 1800 UTC 27 May 1997.

using infrared radiance measurements from the NOAA *GOES-8* sounder. In the sounding, significant low-level moisture was again present (in a deeper layer than 1200 UTC soundings showed) with extreme conditional instability (CAPE exceeding 5000 J kg^{-1} for surface-based parcels), and almost no CIN. Winds were weak in lower levels, but directional shear was substantial in the lowest 300-mb layer. Note that the mean wind in the 0–6-km layer was only around 5 m s^{-1} from 250°.

During the afternoon hours, the convection propagated in a direction strongly deviant from the mean flow, generally toward the south or south-southwest roughly along the prefrontal trough at 5–10 m s^{-1} before developing more of a southeastward component after 0000 UTC 28 May. Additional convection developed southwest of this region in southern Texas, and it had little movement, resulting in the maximum precipitation reported for the event (Fig. 1c), near Cotulla, Texas (COT).

3. Model configuration and design of experiments

For all of the simulations performed, the Eta Model was run with a roughly 2000 km × 2000 km domain located in the central portion of the United States. Initial and boundary condition data were supplied from 80-km Eta datasets generated from the 48-km operational runs and supplied to Iowa State University through the University Corporation for Atmospheric Research Unidata program. To reduce model spinup problems, initialization time was chosen for each case to allow roughly 6–12 h before the primary excessive rainfall event developed. To reduce problems associated with lateral boundaries in the limited domain, however, the simulations were designed so that the precipitation event of interest occurred within the first 18–24 h of integration. For the June 1996 and July 1996 cases where other significant precipitation continued in the domain beyond 24 h, the integrations continued for 36 h to monitor trends in total domain precipitation. Soil moisture and soil temperature data were supplied from NCEP datasets and appeared reasonable based upon crop moisture index values and measured soil temperatures. The version of the model used was comparable to the operational version used in late 1997 and contained the more sophisticated modified Oregon State University parameterization for land surface effects (Chen et al. 1996).

Simulations were run for each case using horizontal resolutions of 12, 22, 39, and 78 km. Vertical resolution was held fixed with 32 model layers having depths ranging from 125 m in the lowest layer to over 1 km at the model top. For some simulations, the KF convective parameterization was substituted for the operational BMJ scheme.

It is worth noting the fundamental differences between the BMJ and KF convective schemes. The BMJ scheme eliminates conditional instability by adjusting the temperature and specific humidities in a vertical column toward reference profiles based upon observations taken by Betts (1986) and Betts and Miller (1986). The reference profiles approximately follow moist adiabats with a minimum in θ_{ES} at the freezing level. The scheme may be activated if a parcel in the lower troposphere (defined here as the lowest 290 mb), when lifted moist adiabatically above cloud base (level with maximum θ_{ES}), is found to be warmer than the environment at a given level. A reference dewpoint profile is constructed by plotting the curve associated with a parcel from that pressure level that would be saturated by lifting the reference temperature profile 50 mb. As temperatures are adjusted higher toward the reference temperature profile, the observed moisture profile at the level with positive CAPE is adjusted toward the reference dewpoint profile (i.e., latent heat release must justify the increase of the temperature). If the atmosphere is drier than the reference profile, the convective scheme does not activate. The reference temperature profile is then cooled and the process repeated. An example of reference temperature and dewpoint curves that might be used in the BMJ scheme can be seen in Fig. 7. If there is never a dewpoint profile associated with a temperature profile that has enough moisture to produce the predicted warming, the scheme does not turn on. The reference humidity profiles are relatively dry (J. Kain 1998, personal communication), so that the scheme tends to remove nearly all of the available moisture when activated, and may minimize the role of grid-resolved precipitation physics. The design of the scheme thus favors activation for cases where substantial low to midlevel moisture is present with positive CAPE; the scheme will often fail to activate when substantial dry air is present aloft, such as with the Miller type I sounding (Miller 1972) frequently associated with severe convection in the central United States. Shallow convection is also taken into account in this scheme, which can redistribute heat and moisture vertically, assisting in the activation of the deep convection component. The BMJ scheme can be thought of as being primarily driven by the thermodynamics at a given model grid point. Vertical motion has no direct impact on the scheme, although it could enhance the activation of the scheme indirectly by moistening the low and middle levels of the atmosphere.

The KF scheme is designed to simulate a vertical rearrangement of mass that eliminates CAPE (Kain and Fritsch 1993). The rearrangement occurs through (i) moist convective updrafts, (ii) moist convective downdrafts, and (iii) dry ascent or descent that locally compensates the moist drafts. The scheme was designed to promote a transition to grid-scale precipitation as the scheme itself removes CAPE. It is worth noting that an additional convective adjustment (following the technique of BMJ) has been developed for use in the KF scheme (J. Kain 1998, personal communication) to prevent a localized response (excessive rainfall) to moist unstable lapse rates in regions of strong ascent. Although the adjustment is used for some sensitivity tests discussed in this paper, the original KF scheme is used for the primary comparisons with the BMJ scheme since the primary purpose of the intercomparison is to investigate QPF-resolution sensitivity in simulations with significantly different convective parameterizations.

Unlike the BMJ scheme, a trigger function based on grid-resolved vertical motion is used to determine activation of the KF scheme. The amount of convective inhibition to be overcome by a parcel (in the lowest 300 mb of the atmosphere) rising from its lifting condensation level to its level of free convection is calculated at each point. The resolvable-scale vertical motion is used to determine a temperature perturbation, which is proportional to $w^{(1/3)}$. If upward motion is large enough to overcome convective inhibition, the scheme will activate (as long as the unstable layer is at least 60 mb deep). A running 10-min mean of the grid-resolved vertical motion is used in the scheme. This ‘‘trigger’’ was originally designed for a 25-km model grid; if the horizontal resolution differs, a linear adjustment is made to the vertical motion to estimate what it would be with a 25-km grid. This linear adjustment should reduce the horizontal resolution dependence of the scheme, although the assumed linear variation may not be entirely accurate, and thus some changes in the KF scheme convective precipitation component may still be expected as resolution changes. In summary, the KF scheme may be more directly influenced by surface convergence and the resulting upward motion features than the BMJ scheme, because the ascent facilitates activation of the scheme. Changes in horizontal resolution and the resulting changes in magnitude of resolved vertical motion could therefore more greatly impact the convective scheme if the changes in vertical motion deviate from the assumed linear adjustment. Of probably more importance, the scheme's design to promote grid-scale precipitation physics should allow the impact of changing horizontal resolution on grid-resolved precipitation to be more easily seen. Finally, for cases where an elevated mixed layer with dry air serves as a capping inversion, inhibiting convective development, the KF scheme will be more likely to activate than the BMJ scheme.

Molinari and Dudek (1992), among others, have raised the concern that convective parameterizations are often designed for a specific range of horizontal resolutions and later applied to resolutions where the physical justification is more questionable. Because a large range of horizontal resolutions is used in this study, the performance of the parameterizations at some resolutions may be less than optimal. However, the range of resolutions has been chosen to represent the general range used operationally and quasi-operationally in the last few years. It is conceivable that each parameterization may exhibit its own response to changes in horizontal resolution. Thus, a goal of this work is to not only study the impact of changes in horizontal resolution and in choice of convective parameterization on QPF independently, but also to note similarities or differences in precipitation trends among the two convective schemes for changing horizontal resolution. The limited sample size will put some constraints on conclusions drawn from the results; however, the analysis and simulation of the three cases should yield some information that can assist forecasters. Although each convective parameterization contains a number of parameters that can be fine-tuned to possibly improve the results (e.g., Vaidya and Singh 1997), the large number of simulations required for this study of three cases made such manipulation unfeasible. It is worth noting, however, that Hong and Pan (1998) have found that even subtle changes within a convective parameterization can have significant impacts on the simulation of precipitation. It was believed to be of greater value in this study to hold most parameters constant among the different simulations, in a manner similar to that used operationally (T. Black 1998, personal communication). Likewise, manipulation of ‘‘tunable’’ parameters to improve results for each particular case and horizontal resolution was not done, as this is not an option in operational runs. It is likely that some improvement could be made by such manipulation in each of the simulations to be discussed.

4. Simulations of excessive rainfall events

a. 16–17 June 1996

1) SIMULATIONS WITH THE BMJ SCHEME

Simulations of the June 1996 flood event were initialized with data from the operational 1200 UTC 16 June Eta run and integrated for 36 h. Total simulated precipitation for the 24-h period shown in Fig. 1a (1200–1200 UTC) over roughly the same region of in-

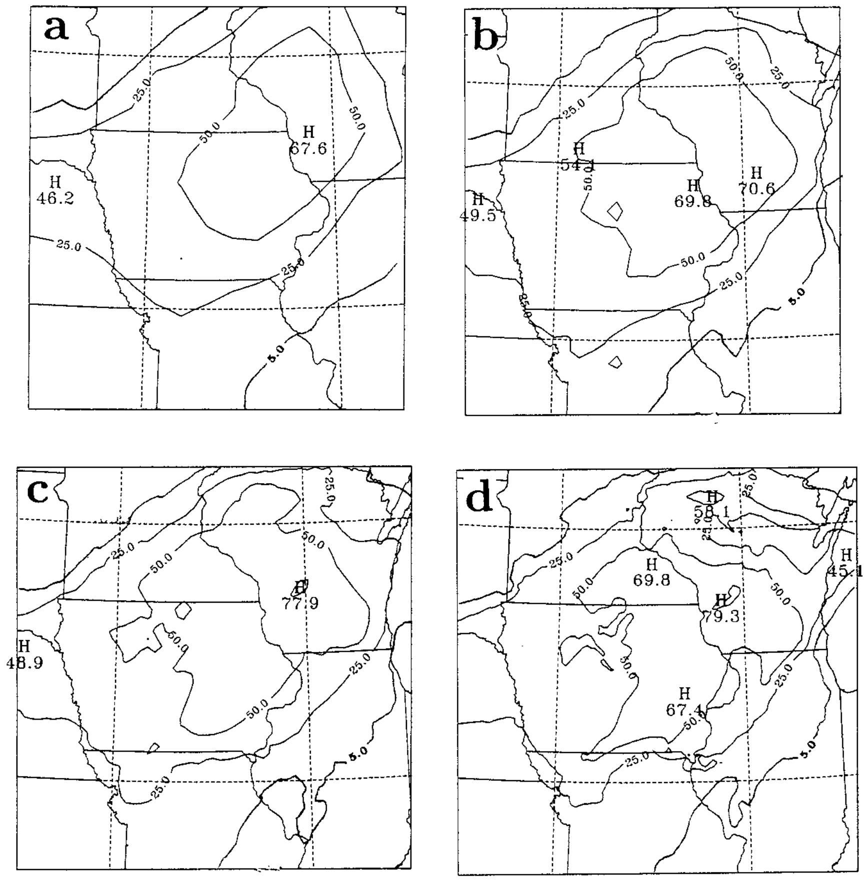

FIG. 10. Eta Model (with BMJ convective parameterization) accumulated precipitation (mm) for the 24-h period 1200 UTC 16 Jun–1200 UTC 17 Jun 1996 for horizontal resolutions of (a) 78, (b) 39, (c) 22, and (d) 12 km. First contour is 5 mm; otherwise contour interval is 25 mm.

terest for runs with 78-, 39-, 22-, and 12-km horizontal resolution using the BMJ convective parameterization can be seen in Fig. 10. Somewhat surprisingly, the general QPF field shows little variation among these different simulations (although finer-scale variations within the main precipitation region can be seen at higher resolutions). In all cases, significant rainfall is shown for all of Iowa and nearby states, with the axis of heaviest rainfall from northeastern Nebraska northeastward into Wisconsin, where peak 24-h totals range from 67.6 mm in the 78-km horizontal resolution run to 70.6 mm in the 39-km run, 77.9 mm in the 22-km run, and 79.3 mm in the l2-km run. In all four simulations, at least 85%–90% of the precipitation in the region of greatest amounts (and in general throughout the region shown in Fig. 10) was produced by the convective scheme. As stated earlier, an extensive area of heavy rainfall, averaging at least 50–100 mm, did occur north of the warm front in Wisconsin during this period. Thus, all of the simulations did a reasonable job of indicating the likelihood for large totals there. Apparently the supply of moisture and low-level convergence allowing upward vertical transport of moisture for this heavy rain event was of sufficiently large scale so that the BMJ scheme produced similar amounts of precipitation at all four resolutions. With the significant drying of the atmosphere produced by the BMJ scheme, grid-resolved precipitation was small, and little change occurred in total precipitation as model resolution varied from 78 to 12 km.

Farther south, however, all four simulations failed to indicate the much smaller-scale region of excessive rainfall that developed in central Iowa. Since the entire region experiencing greater than 100 mm of rainfall was confined to a band no more than 30 km wide by 60 km long (Fig. 1a), it is understandable that the coarser-resolution simulations would fail to capture this event. Although the 12- and 22-km runs would not fully resolve the band, the fact that these finer-resolution runs failed to show any significant enhancement in precipitation within the warm sector is not as easily explained.

As discussed previously, early morning convection had occurred across much of Iowa and may have left an outflow boundary in its wake over central Iowa (Fig. 3). Convective boundaries are known to play an important role in the formation of convection, and reduced

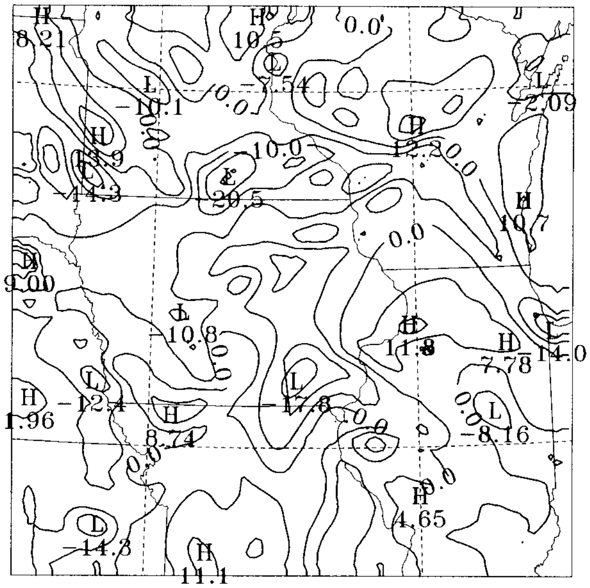

FIG. 11. Eta Model moisture divergence ($\times 10^{-4}$ g kg^{-1} s^{-1}) at 2100 UTC 16 Jun from a 12-km horizontal resolution run. Contour interval is 5×10^{-4} g kg^{-1} s^{-1}.

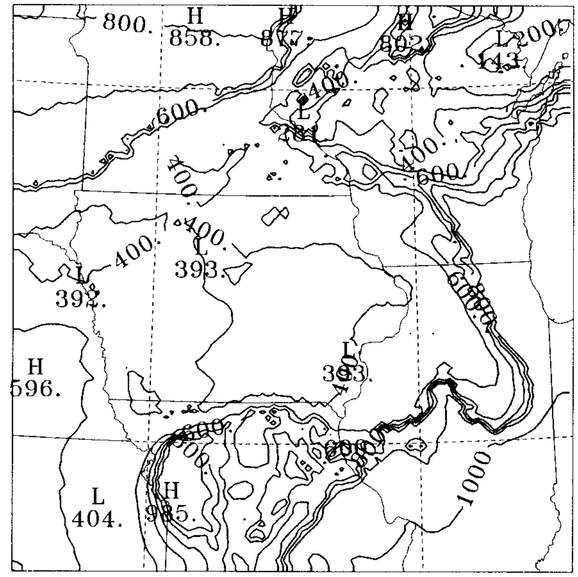

FIG. 12. Shortwave solar irradiance (W m^{-2}) at the surface at 1800 UTC in the 12-km Eta simulation. Contour interval is 100 W m^{-2}.

model precipitation skill scores associated with warm season precipitation have been attributed to model difficulties in producing or maintaining these small-scale boundaries (Schneider et al. 1996). In fact, the surface wind field at model initialization (taken from the 0-h forecast of the 1200 UTC 16 June Eta Model) showed southerly winds across all of southern Iowa, when actual observations indicated a significant easterly component due to the ongoing MCS at 1200 UTC in eastern Iowa (not shown). The inadequate initialization of a preexisting cold pool could adversely affect the simulated wind fields later in the day. Stensrud and Fritsch (1994a,b) noted the importance of adequate initialization of mesoscale features for convective precipitation forecasting and found that mesoscale initialization was of particular importance for systems occurring in weakly forced large-scale environments. Although a significant amount of large-scale forcing was present in the upper Midwest on 16 June, it can be argued that this forcing was relatively weak in central Iowa during the afternoon hours, when the larger-scale fronts were to the north and west.

Although the surface wind field in the model at 1200 UTC did differ significantly from actual observations in parts of Iowa, the simulations did show a moisture convergence pattern at 2100 UTC (Fig. 11) in some agreement with observations (Fig. 4). The general pattern of moisture convergence in Iowa could be seen at all four horizontal resolutions, but was most pronounced with the highest-resolution version of the model (12 km), shown in the figure. Significant moisture convergence was present near Iowa's northern border along the warm front (displaced ~100 km north in the model from observations), in southeastern Nebraska near the cold front or trough, in parts of eastern Iowa, and in a small region of west-central Iowa, where the actual flood-producing convection developed around this time (accounting for the small area of moisture divergence observed in west-central Iowa). Although the higher resolution of the model data compared to observations must be taken into account when comparing magnitudes of the fields, it is apparent that the model actually simulated more pronounced moisture convergence in west-central and southeastern Iowa than that observed. In spite of the enhanced convergence in west-central Iowa, no significant precipitation was generated in the model simulations there around or after this time. This result implies that perhaps the inadequate depiction of leftover boundaries was of secondary importance in the failure to simulate the small-scale maximum in precipitation in central Iowa. Of potentially more importance may have been an underestimate of instability in the model due to overpredicted cloudiness throughout the day.

As shown in Fig. 3 (and supported by satellite imagery), skies had partially cleared by midday (1800 UTC) in much of southern Iowa, allowing afternoon temperatures to later rise above 27°C. The shortwave irradiance reaching the surface at 1800 UTC in the l2-km run can be seen in Fig. 12. In the simulation, extensive cloud cover (~60% reduction in irradiance) remained across all of Iowa throughout the day (some partial clearing is present in northern Missouri). Lowest model layer temperatures (~surface air temperatures) were correspondingly reduced by the smaller sensible heat flux and were around 2°–4°C lower than observed values during the afternoon (dewpoint temperatures were in closer agreement with observations). It is pos-

TABLE 1. Domain-integrated total precipitation (10^{12} kg) for the Eta simulations for 16–17 Jun 1996 using the BMJ scheme.

Time (h)	78 km	39 km	22 km	12 km
6	10.4	9.7	9.4	9.1
12	18.2	17.4	17.0	16.6
18	23.1	22.4	22.1	21.6
24	27.0	26.7	26.4	25.8
30	31.1	31.1	30.9	30.5
36	36.6	36.7	36.5	36.3

sible that the resulting reduction in instability played a role in the failure of the model to generate heavy precipitation, even in the 12-km resolution version.

In summary, for this case, with the operational BMJ convective parameterization, horizontal resolution had little effect on the QPF. All runs showed extensive heavy precipitation north of the warm front in Wisconsin, and all runs would require similar adjustment of the precipitation amounts to accurately forecast the extent of the excessive rainfall there. In addition, all runs failed to simulate excessive rainfall in central Iowa, limiting the usefulness of this guidance supplied to operational forecasters. The relative insensitivity to horizontal resolution can also be seen in the domain-integrated total precipitation during the 36-h simulation (Table 1). Through 30 h of simulation, there was a small tendency for total domain precipitation to decrease with increasing horizontal resolution, but the reduction as resolution improved from 78 to 12 km never exceeded 13%. The largest reduction occurred during the first 6 h of simulation and may have been caused by different spinup behavior (Molinari and Dudek 1992) for different horizontal resolutions (e.g., Gallus and Bresch 1997). The reduction decreased with time. By 36 h, the total precipitation in the domain varied by less than 2% between all four of the horizontal resolutions tested. The general, although small, increase in peak QPF that occurred with increasingly fine resolution was not accompanied by an increase in the total domain precipitation for this case.

2) COMPARISON OF SIMULATIONS WITH THE KF AND BMJ SCHEMES

The above simulations were repeated at the same four horizontal resolutions with the KF convective parameterization, which is designed to allow more of the removal of CAPE to occur on the grid scale, thereby improving the likelihood that grid-resolved physics will play an important role in simulating realistic mesoscale features. In these simulations with the KF scheme, more significant changes than in the BMJ runs occurred in the rain region as resolution improved (Fig. 13), particularly within the warm sector from Iowa southward. Along or north of the warm front in Wisconsin, the general pattern of rain did not change significantly, but the peak precipitation was more sensitive to the resolution than that found with the BMJ scheme. In this region, peak rainfall of 68 mm at 78-km resolution increased to 121 mm at 39-km resolution, and then fluctuated slightly to 116 mm at 22-km resolution and 127 mm at 12 km. Unlike in the BMJ simulations, the precipitation maxima here in the KF runs were almost entirely grid resolved. Therefore, the almost doubling in peak QPF as resolution increased from 78 to 39 km probably reflected the impact of stronger resolved vertical motion on grid-resolved precipitation. The lack of further increase at even higher resolution was likely related to changes occurring in the warm sector precipitation.

As stated above, the largest changes in this set of simulations occurred within the warm sector. At horizontal resolutions of both 78 and 39 km, peak warm sector precipitation was roughly 30 mm, and most of this precipitation was produced by the convective scheme. At 22-km resolution, significant increase occurred in QPF in several regions, most noticeably near central Iowa where 101 mm was simulated in a region that had less than 50 mm simulated at 39 km. Precipitation in this small region continued to increase dramatically as resolution was refined to 12 km, with 184 mm occurring. At 22 and 12 km, most of this precipitation, although occurring in the more unstable warm sector, was grid resolved. The KF scheme did activate, and as originally designed, it allowed much of the removal of CAPE to occur on resolved scales, so that refinements in horizontal resolution had large impacts on QPF. Total domain precipitation in these simulations (Table 2) was roughly 50% or more lower than with the BMJ scheme (Table 1) through the first 12 h, and from 20% (high-resolution runs) to nearly 40% (low-resolution runs) lower later in the simulations. Unlike in the BMJ runs, this quantity did change appreciably as resolution was varied, with a general 25% increase as resolution improved from 78 to 12 km.

The high-resolution KF runs appear to roughly capture the excessive rainfall event that occurred within the warm sector in central Iowa. Most of the model rain occurred during a period of only 6 h, roughly from 0300 through 0900 UTC. The precipitation maximum was thus displaced a small distance eastward from the actual event and delayed a few hours in time. These runs also produced separate precipitation maxima to the southwest toward northwestern Missouri where enhanced precipitation had been observed. However, the model also simulated small-scale precipitation extrema where none were observed (e.g., western Illinois).

It is difficult to evaluate whether the small-scale precipitation extrema that develop in the 22- and 12-km KF runs constitute an improved forecast. The issue is somewhat a subjective one. In many cases, these extrema from gridpoint-like storms would be considered highly undesirable. Because of this, an adjustment to the KF scheme has been developed (J. Kain 1998, personal communication) for possible use operationally that allows an additional convective adjustment pro-

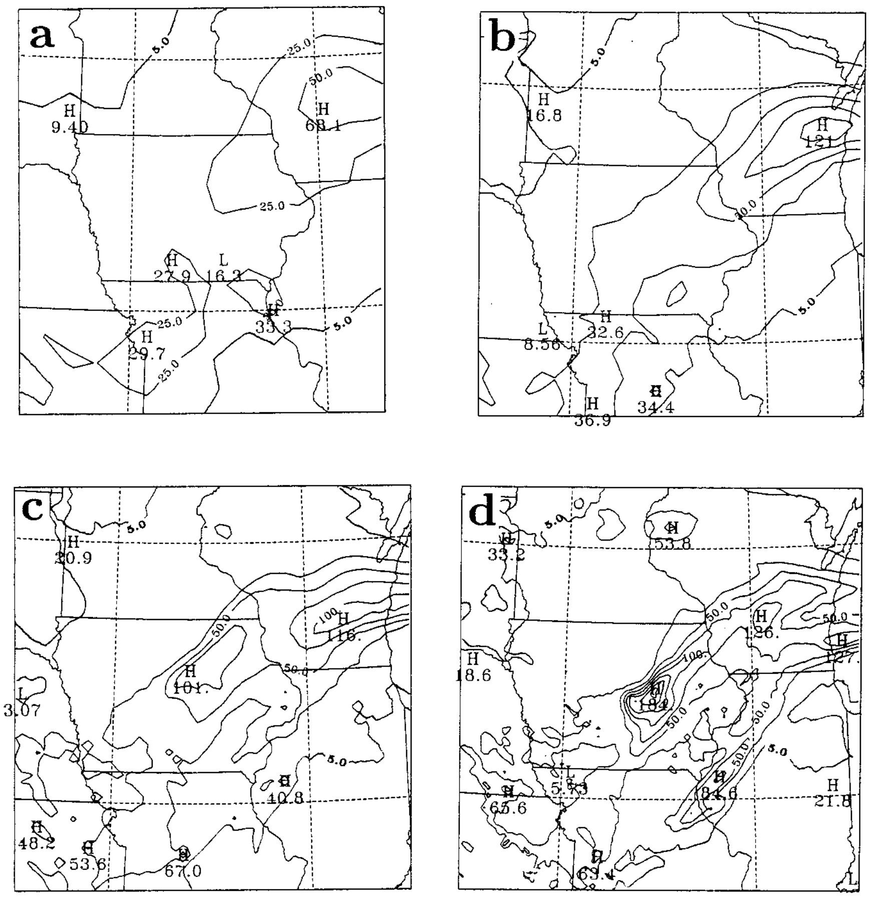

FIG. 13. As in Fig. 10 but for the KF scheme.

cedure (similar to that used in the BMJ scheme) to activate when the model shows signs of a localized response to moist, unstable lapse rates. The additional adjustment is designed to dampen excessive localized rainfall that may occur. The above simulations were repeated with that additional adjustment, and no significant enhancement of warm sector precipitation developed. Interestingly, without the excessive rainfall in Iowa, the peak precipitation in those runs, almost entirely grid resolved and located in Wisconsin, continued to increase as resolution improved (instead of fluctuating at 22 and 12 km as described earlier). This strongly indicates the complex interaction that occurs between grid-resolved and convective precipitation, even at grid points rather far apart. Total domain precipitation with the adjustment was an additional 10%–20% smaller than that in the BMJ runs.

TABLE 2. Domain-integrated total precipitation (10^{12} kg) for the Eta simulations for 16–17 Jun 1996 using the KF scheme.

Time (h)	78 km	39 km	22 km	12 km
6	3.0	3.2	3.1	2.8
12	8.0	8.6	9.0	8.4
18	12.2	13.6	15.0	14.5
24	15.6	17.6	19.8	19.8
30	18.4	20.9	24.1	24.0
36	23.4	25.7	29.4	28.9

An additional significant difference between the BMJ and KF parameterizations is in the precipitation produced during the first 6 h of integration. As mentioned earlier, an MCS was traveling east from central Iowa at 1200 UTC 16 June. The system dissipated during the next 6 h. In simulations with the BMJ scheme, a large amount of precipitation was produced over all of Iowa and nearby states during the first 6 h of integration. The QPF field from the 22-km run can be seen in Fig. 14a. Most of this precipitation was produced by the convective parameterization. Simulations with the KF scheme, however, produced a much smaller area of precipitation during these first 6 h (Fig. 14b), most of which again was from the convective scheme, and agreed better with observations of a dissipating convective system moving eastward. Convective regeneration in western Iowa was not observed to occur until after 1800 UTC. It is likely that the different criteria used to trigger activation of the parameterizations resulted in the significant differences in QPF during the 1200–1800 UTC time period. In this particular case, the BMJ dependence on signif-

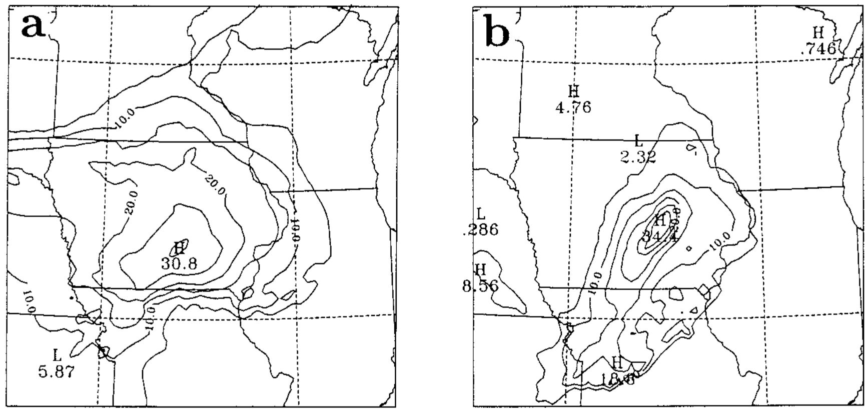

FIG. 14. Accumulated precipitation (mm) in 6-h period (1200–1800 UTC 16 Jun) from the 22-km Eta Model with the (a) BMJ and (b) KF convective parameterizations. Contour interval is 5 mm.

icant amounts of moisture in a deep lower-tropospheric layer may have been too lenient a ''trigger,'' resulting in significant precipitation over a broad region.

b. 16–17 July 1996

1) SIMULATIONS WITH THE BMJ SCHEME

The QPF in the July 1996 MCS simulations behaved somewhat differently than in the 16 June simulations. Figure 15 shows the 24-h QPF from 78-, 39-, 22-, and 12-km horizontal resolution versions of the model with the BMJ scheme, valid for the period ending at 1200 UTC 17 July. This model version simulated well the occurrence of a convective precipitation area in western Iowa during the 0000–1200 UTC 17 July time frame. However, the peak amounts were severely underestimated (the scheme also produced too much precipitation too early in Nebraska, prior to 0000 UTC 17 July). Peak rainfall in western Iowa was 46.1 mm in the 78-km resolution case, 44.8 mm in the 39-km version, and 31.9 mm in the 22-km version. As resolution improved further to 12 km, the peak amount rose to 37.4 mm in a location somewhat farther south, while staying about the same, 32 mm, near southwestern Iowa. Thus, a significant *reduction* in peak predicted precipitation generally occurred as horizontal resolution was refined (from 78 to 22 km). Interestingly, the domain total precipitation increased significantly over this time as the resolution improved (Table 3). Both of these results are opposite to those found in the 16 June case. Once again, nearly all (>98%) of the precipitation in Iowa was produced by the convective scheme in all four simulations. The dominance of convective precipitation (and the pronounced effect the BMJ scheme has on moisture profiles) prevented a significant contribution from the grid scale, likely explaining the failure of higher-resolution runs to develop larger precipitation totals.

2) COMPARISON OF SIMULATIONS WITH THE KF AND BMJ SCHEMES

In a set of tests where the KF scheme was substituted, results changed dramatically, with the location of the precipitation region in less agreement with observations than in the BMJ runs, but the amounts being more reasonable. The 24-h QPFs from the KF runs at 78-, 39-, 22-, and 12-km resolutions can be seen in Fig. 16. In this case, the model did not develop significant precipitation during the daylight hours of 16 July well west into Nebraska, a result agreeing better with observations. However, the precipitation that developed after 0000 UTC occurred too far north. In sharp contrast to the BMJ runs, the peak precipitation increased greatly with increasing resolution, from around 10 mm in the 78-km run to 70 mm in the 39-km run, 135 mm in the 22-km run, and 186 mm in the 12-km run. Similar to the 16 June case, the KF convective scheme in the higher-resolution runs contributed a much smaller fraction to the total precipitation in the region of highest amount than the BMJ scheme had. In the 78-km run, all of the precipitation was due to the KF parameterization. The fraction decreased to 15% at 39 km, and to under 10% at 22 and 12 km. At the higher resolutions where large amounts of rain were simulated, most of the precipitation to the south of the maxima (where amounts were light) was produced by the convective scheme. A rapid transition to primarily grid-resolved precipitation occurred just south of the maxima. The domain precipitation increased even more rapidly than in the BMJ runs for increasingly high resolution in this case (Table 4). The domain total with 39-km resolution was over double that with 78-km resolution, and the amount continued to increase substantially as resolution changed from 39 to 22 and 12 km.

The much larger rainfall amounts in the KF scheme were certainly much closer to observed amounts, as several locations in west-central Iowa measured over 300

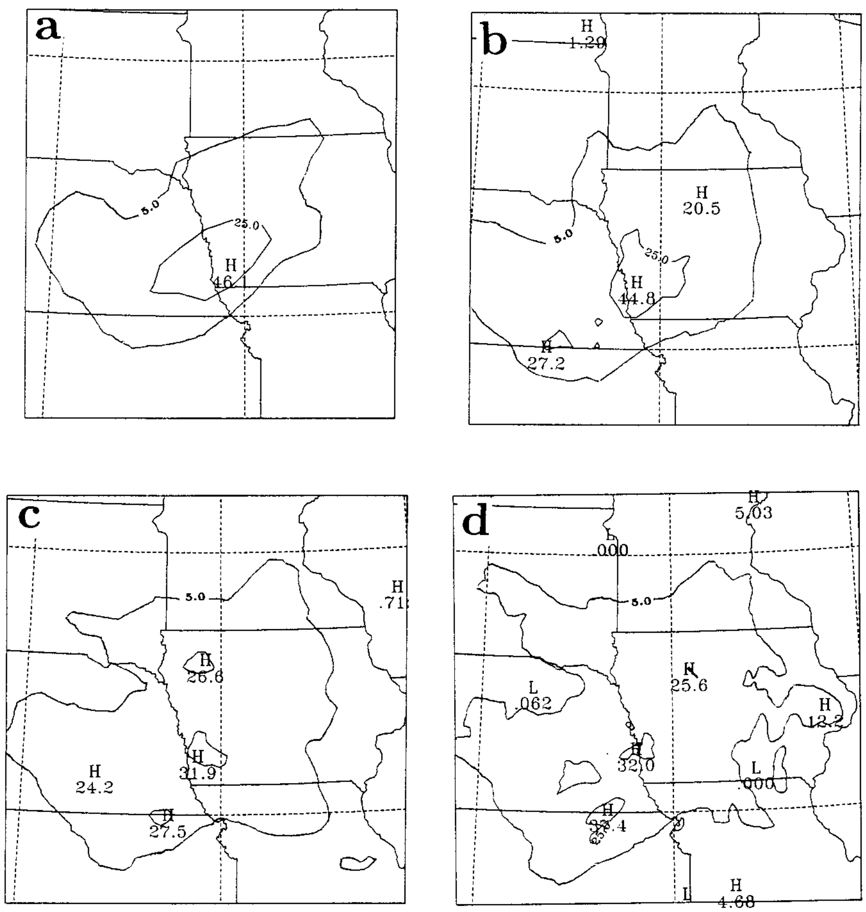

FIG. 15. As in Fig. 10 except for the 24-h period 1200 UTC 16 Jul–1200 UTC 17 Jul 1996.

mm. However, spatial errors were worse. Of note, when the additional convective adjustment was used in the KF scheme (figures not shown), peak rainfall amounts were reduced somewhat (~20%–50%), and the main precipitation band across central Minnesota shifted southward by roughly 50 km. For this event, significant contributions from the convective scheme appeared to be necessary to result in a farther southward precipitation maximum.

The unusual behavior of the QPF for the two schemes in this case requires some effort to explain. With less relative humidity in much of the lower troposphere than in the June case, and a pronounced warm frontal boundary serving as an overrunning surface, it might seem the KF scheme should be favored for activation compared to the BMJ scheme, particularly with a layer of dry air just above 700 mb (Fig. 7) and relatively warm air at 700 mb advecting northward. Yet, nearly all of the precipitation in the BMJ runs was produced by the convective scheme, and most of the precipitation in the region of highest amounts in the KF runs was grid resolved.

TABLE 3. Domain-integrated total precipitation (10^{12} kg) for the Eta simulations for 16–17 Jul 1996 using the BMJ scheme.

Time (h)	78 km	39 km	22 km	12 km
12	2.0	2.7	3.0	3.1
24	4.2	5.3	5.8	6.0
36	9.2	10.9	12.1	12.5

As stated earlier, the BMJ scheme activated quickly in this case (as in the June case), producing significant rainfall in much of central and eastern Nebraska prior to 0000 UTC (Fig. 17a). This convective system was able to continue progressing eastward across Iowa during the night. Although the observed Omaha sounding at 0000 UTC (Fig. 7) had lower relative humidity than present in the June case, the actual moisture content was generally just as high (precipitable water was within 10% of the June case). The dry layer above 700 mb was both rather shallow and somewhat elevated, so that detrimental effects for the BMJ scheme were somewhat minimized. The activation of the scheme prior to 0000 UTC in Nebraska generally removed this dry layer. Simulated soundings in central Iowa at 0000 UTC (not shown) indicated nearly saturated conditions with an almost moist-adiabatic temperature profile through much of the depth of the atmosphere, especially above

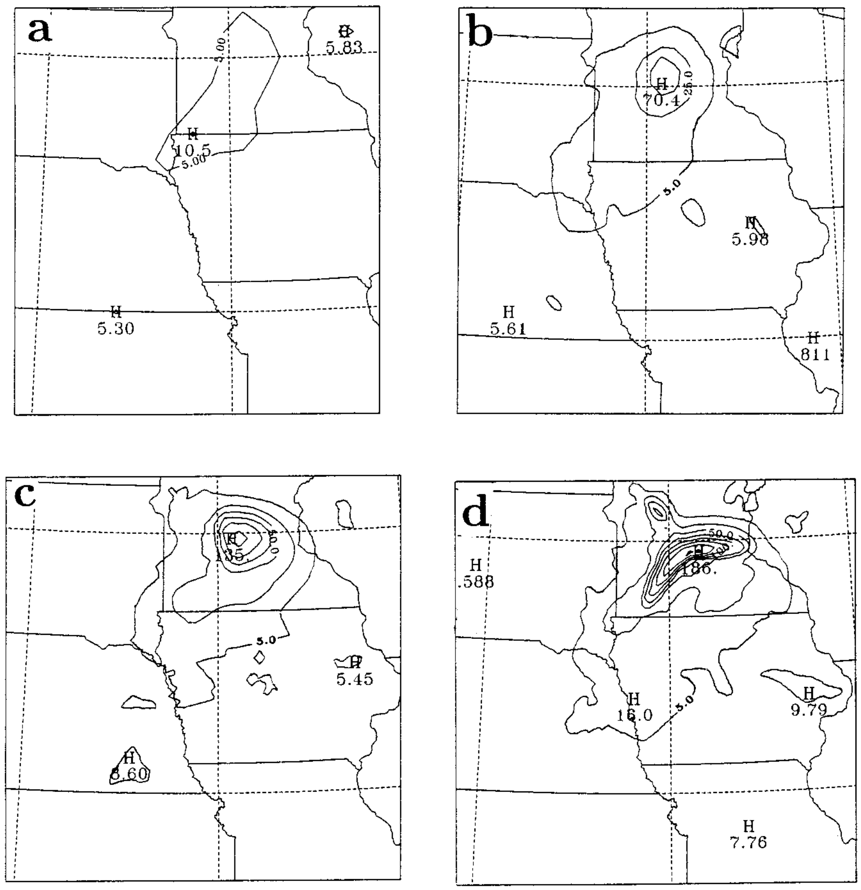

FIG. 16. As in Fig. 15 except for the Eta Model with the KF convective parameterization.

600 mb. Although conditional instability was limited, the moist conditions at midlevels helped the BMJ scheme to activate in this region. Because only modest instability was present, as in the June case, little or no grid-resolved precipitation was able to supplement the convective component.

Different circumstances were present in the KF simulations. Some convection did develop during the afternoon hours prior to 0000 UTC in eastern Nebraska and western Iowa (Fig. 17b), but due to limited instability in this region, rainfall amounts were small (under 6–8 mm). The convection was relatively high based, and surface divergence associated with the convection was much stronger than in the BMJ runs (because of the parameterized downdrafts in the KF scheme), resulting in a stronger push of moisture northward into southern Minnesota, and a much tighter thermal boundary there (figure not shown). Conditions in southern Minnesota were much warmer than in Iowa in both sets of simulations (around 31°C) due to cloud cover differences. The stronger low-level convergence with greater moisture in far southern Minnesota may have assisted in triggering convection there.

A comparison of model soundings from the 22-km BMJ (Fig. 18a) and KF (Fig. 18b) runs valid in southwestern Minnesota at 0000 UTC shows more favorable conditions for convection in the KF runs. Boundary layer moisture was deeper, possibly due to the stronger low-level convergence. Of potentially more importance, conditions were significantly moister aloft with substantially different winds than in the BMJ runs. It appears as though the large region of daytime precipitation over Nebraska in the BMJ runs may have altered the general southwesterly flow. The layer from roughly 600 to 850 mb in the BMJ runs had some easterly component (Fig. 18a). In the KF runs, no easterly component occurred in this layer, and moisture advection from the south-southwest was greater, probably accounting somewhat for the moister conditions. In addition, the lifting condensation level for surface-based parcels was very

TABLE 4. Domain-integrated total precipitation (10^{12} kg) for the Eta simulations for 16–17 Jul 1996 using the KF scheme.

Time (h)	78 km	39 km	22 km	12 km
12	3.0	3.6	3.0	2.8
24	3.7	5.9	7.0	7.7
36	5.4	11.0	13.5	14.1

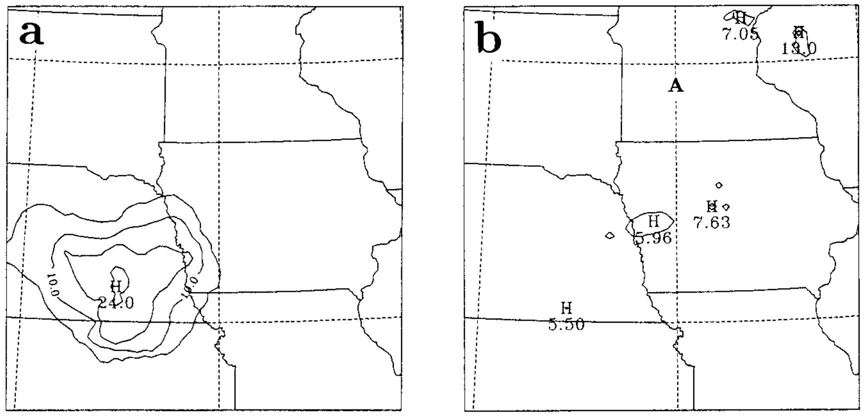

FIG. 17. As in Fig. 14 except for the 12-h period from 1200 UTC 16 Jul–0000 UTC 17 Jul.

close to the level of free convection in the KF runs. The upward motion associated with the low-level convergence would have little difficulty activating the scheme. The relatively dry conditions found in the BMJ runs would make activation of the BMJ scheme difficult. A strong low-level jet developing during the nighttime hours continued to supply significant moisture, allowing heavy grid-resolved precipitation to occur in the KF runs in conjunction with the KF convective component (the convective component was concentrated on the south side of the precipitation maximum).

It should be noted that both sets of simulations incorrectly simulated the boundary layer evolution in parts of southwestern Minnesota. Observed temperatures at the location of the soundings in Fig. 18 were around 26°C, or roughly 4°C lower than the model predicted. Warmer conditions were observed to the north. The model apparently eroded a mesoscale cool pool too quickly from the north and northeast in Minnesota, resulting in an incorrect depiction of the preconvective environment, with unrealistic destabilization of the boundary layer too far southwest into southern Minnesota. In real time, forecasters can easily evaluate whether or not the general evolution of surface features within a mesoscale prediction actually matches observations.

Simulations with both the BMJ and KF schemes showed cool, relatively stable air over western Iowa, similar to the observations at 0000 UTC (Fig. 6). Neither scheme seemed to correctly predict the strong overrunning of the boundary that would produce the flooding rains in Iowa. The BMJ scheme did show substantial rainfall, but it seemed to be more related to an existing convective system that propagated eastward. The KF scheme did produce a heavy nocturnal precipitation event, but with significant displacement northward from observations, either due to the inaccurate prediction of afternoon convection in Iowa, or perhaps inaccurate simulation of the strongest convergence associated with the low-level jet that developed after 0000 UTC. Not surprisingly, with incorrect simulation of the general MCS evolution, neither scheme simulated well the southeastward observed movement of the heaviest rainfall elements within the MCS.

c. 27 May 1997

The excessive rainfall in the 27 May case was less intense and covered smaller areas than the other two cases, and as would be expected, the sensitivity of QPF to horizontal resolution and convective parameterization again differed substantially from the other cases. Convection generally dissipated by 0600 UTC 28 May, and simulations were therefore only run for 18 h. This case also exhibited the most extreme instability of the three cases.

1) SIMULATIONS WITH THE BMJ SCHEME

Figure 19 depicts the 18-h QPF for the period from 1200 UTC 27 May through 0600 UTC 28 May for model runs with horizontal resolutions of 78, 39, 22, and 12 km, using the BMJ convective scheme. Peak amounts were only around 10 mm at 78-km resolution, but increased to 28 mm at 39-km, 102 mm at 22-km, and 203 mm at 12-km resolution. Over 90% of the precipitation was produced by the convective scheme for resolutions of 78 and 39 km. At finer resolutions, the convective component of the precipitation remained around 30 mm, so that the significant increases in precipitation were primarily due to increased grid-resolved precipitation. The maximum precipitation occurred within a gridpoint stormlike system near the Rio Grande River in south-central Texas.

The behavior of the BMJ convective scheme in this case was significantly different than in the other two cases. In the May case, the convective scheme was not able to suppress the grid-resolved precipitation as it did in the previous two cases. Grid-resolved precipitation was significant, and thus a large QPF-horizontal resolution dependence existed. The primary difference between the environment of the May case and that of the

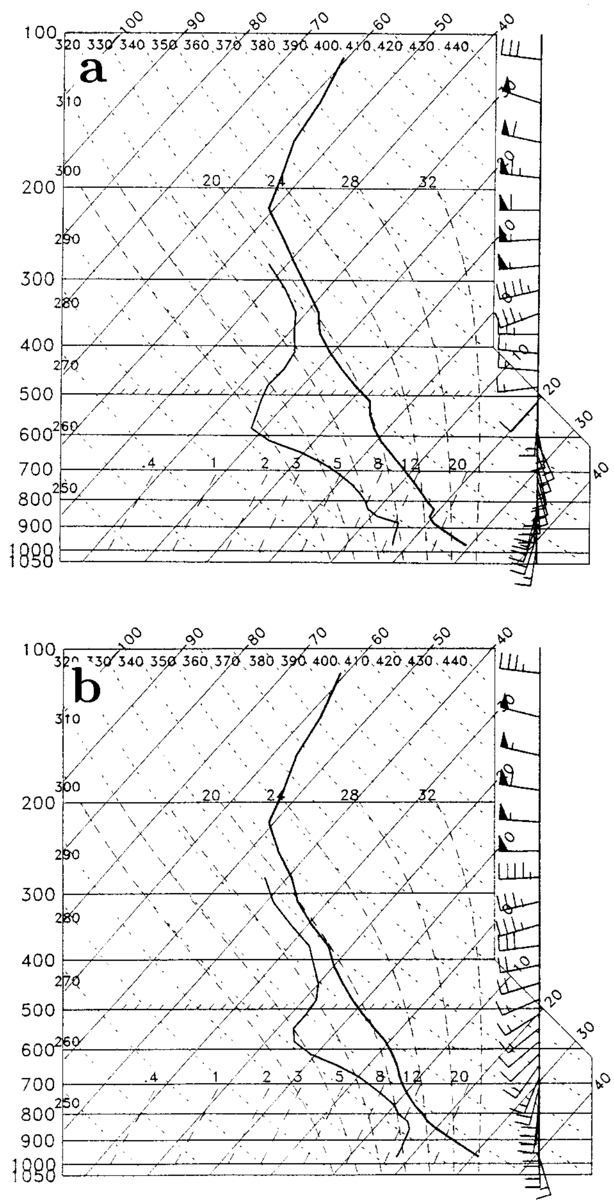

FIG. 18. Model skew *T*–log*p* diagrams for a point in southwestern Minnesota (labeled A in Fig. 17b) at 0000 UTC 17 Jul for the 22-km Eta with (a) BMJ and (b) KF convective parameterizations.

others was in the degree of conditional static instability of the atmosphere. This result suggests that for ''aggressive'' convective schemes that tend to significantly diminish the grid-resolved precipitation component, the expected increase in QPF as resolution improves may be most likely in environments of substantial conditional static instability.

The model results with the BMJ scheme were in reasonable agreement with observations (Fig. 1c), in terms of the general location and timing of the precipitation event. Peak amounts were underestimated by the 78- and 39-km resolution simulations; however, the grid-point storm feature at higher resolutions resulted in model QPF at 22 km similar to the maximum observed and a significant overestimate at 12 km. Total domain precipitation behaved similarly to the peak QPF, with marked increases as resolution improved (Table 5). The general increase was similar to the 16–17 July case, with the largest increase occurring as resolution improved from 78 to 39 km. The total with 12-km resolution was nearly three times as large as with 78-km resolution.

Interestingly, the model generated a southwestward propagating boundary in east-central Texas during the first few hours of simulation, apparently triggered by convective precipitation there. The boundary can be seen in the moisture convergence field at 1500 UTC (Fig. 20). This boundary eventually reached the larger-scale moisture convergence located along the front in central Texas (around 1800 UTC), and heavy precipitation developed around that time. As stated earlier, observations indicated a gravity wave propagated southwestward from early morning convection over Arkansas. A more thorough investigation of model output showed that the simulated boundary behaved more like a density current or outflow boundary as opposed to a gravity wave. Strongest negative U perturbations coincided with a strong pressure gradient behind the southwestward propagating wind shift. An expanding area of low-level divergence trailed the boundary. Of note, only a small amount of cooling occurred at the surface as the boundary passed; however, significant cooling occurred behind the boundary in the lower troposphere, generally in the 0.8–3-km layer (not shown). This somewhat elevated cold pool was likely an artifact of the temperature adjustments occurring in the convective scheme (cloud base was very low). A decrease in temperature can occur in some layers when the BMJ scheme activates, particularly layers with inversions, as long as net latent heat release exists in the vertical column. Although the BMJ scheme does not include the effects of convective downdrafts directly and, therefore, may encounter problems for case where thunderstorm-produced surface cold pools are important, the evaporation of the smaller grid-scale component rainfall, along with reduced solar irradiance reaching the surface, can also result in a pool of somewhat cooler air at the surface that behaves similarly to a typical cold pool. The boundary induced strong upward motion (exceeding 20 μb s^{-1}), which deepened the moist layer from northeast to southwest. The boundary gradually slowed during the 1–5-h time period (1300–1700 UTC) as it approached the larger-scale front, and the persistent strong ascent and deepening moist layer that occurred in this region (near Waco) may have been instrumental in the model's reasonable simulation of the ensuing heavy convective precipitation event.

2) COMPARISON OF SIMULATIONS WITH THE KF AND BMJ SCHEMES

When the KF scheme was substituted in simulations at 78, 39, 22, and 12 km (Fig. 21), the results again

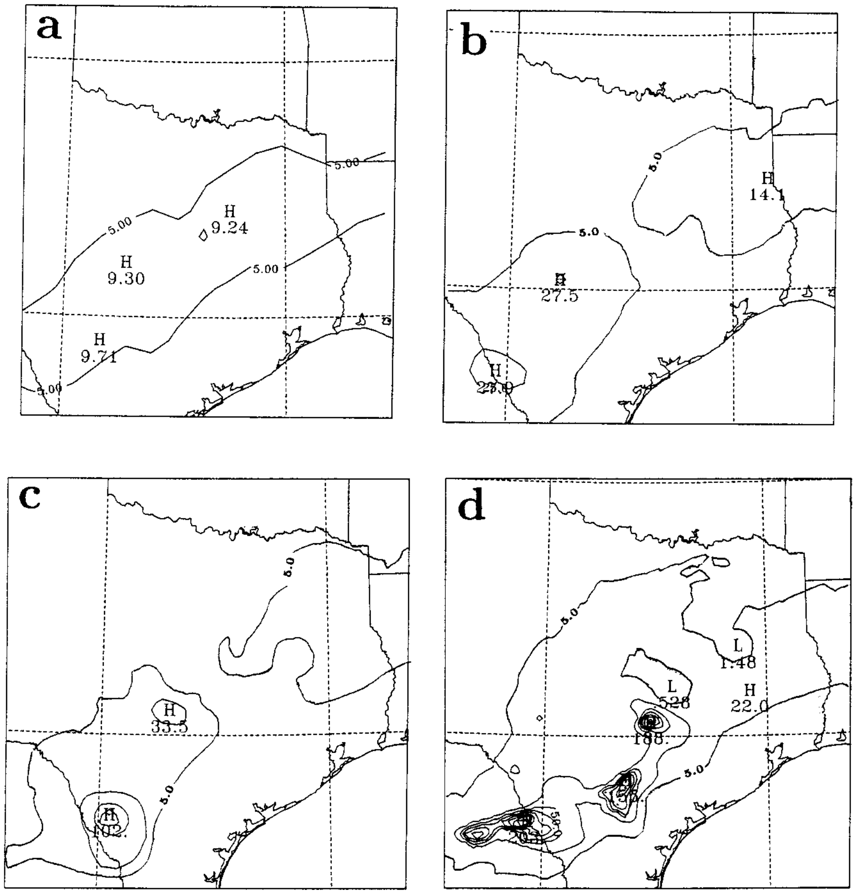

FIG. 19. As in Fig. 10 except for the 18-h period 1200 UTC 27 May–0600 UTC 28 May 1997.

differed dramatically from the BMJ scheme (Fig. 19). In this case, the convective scheme activated early, probably because of the strong moisture convergence and upward motion along the front in Texas. By 1800 UTC, precipitation was produced in the model all along the front (Fig. 22). Observations and the BMJ simulations do not show significant precipitation by this time much southwest of the 9.67-mm maxima in northeastern Texas (see Fig. 22). A more concentrated and organized convective system in south-central Texas generally was not simulated in the KF runs. The precipitation was more uniform along the front without pronounced regions of localized heavy rainfall. In addition, the sensitivity of peak QPF to horizontal resolution was not as strong. Peak rainfalls of 17 mm at 78 km (twice as much as with the BMJ scheme) changed little at 39 km (20 mm) and then only slightly more at 22-km resolution (31 mm)

TABLE 5. Domain-integrated total precipitation (10^{12} kg) for the Eta simulations for 27–28 May 1997 using the BMJ scheme.

Time (h)	78 km	39 km	22 km	12 km
12	2.8	4.3	5.1	5.9
18	5.1	8.2	10.2	13.1

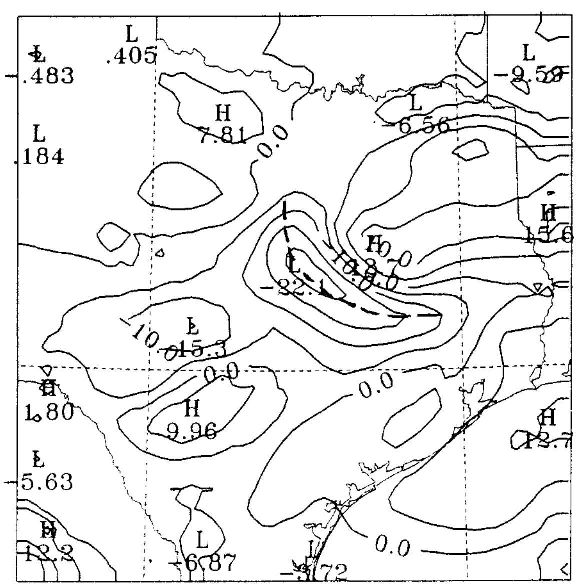

FIG. 20. Eta Model moisture divergence ($\times 10^{-4}$ g kg^{-1} s^{-1}) at 1500 UTC 27 May 1997 from a 22-km horizontal resolution run. Contour interval is 5×10^{-4} g kg^{-1} s^{-1}. Apparent mesoscale boundary indicated with a dashed line.

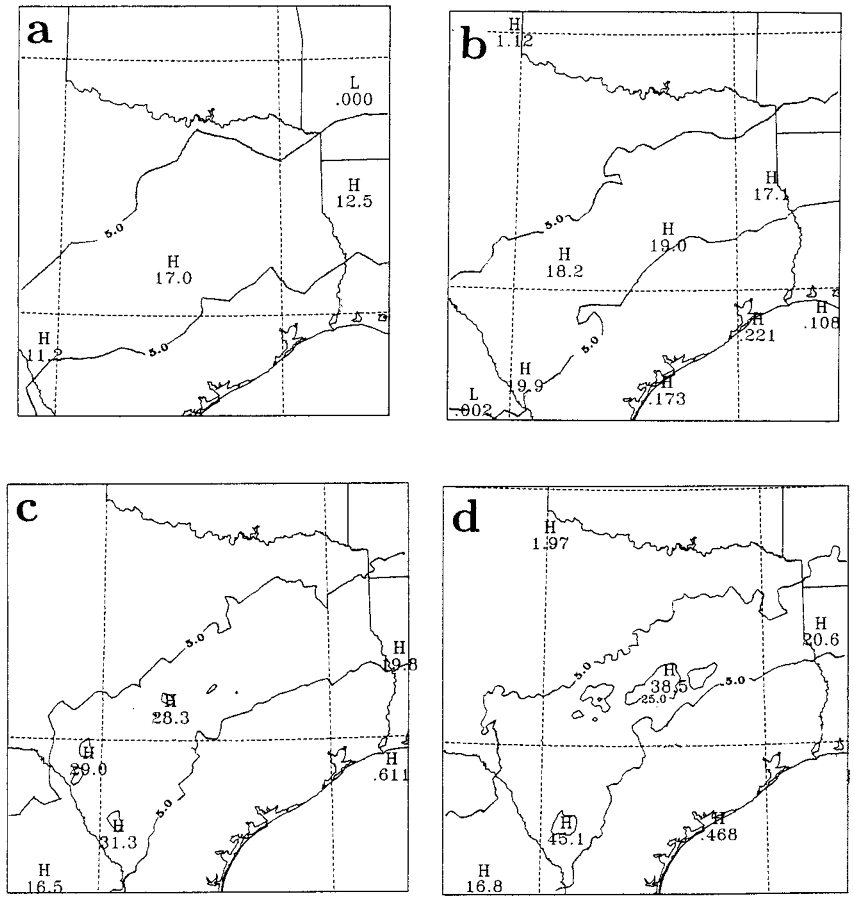

FIG. 21. As in Fig. 19 except for the Eta simulations with the KF convective parameterization.

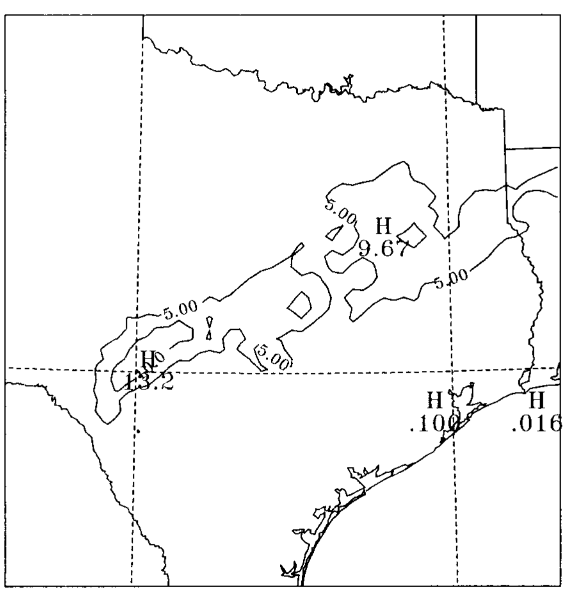

FIG. 22. Accumulated precipitation (mm) in the 6-h period (1200–1800 UTC 27 May) from the 22-km Eta Model with the KF convective parameterization. Contour interval is 5 mm.

and 12-km resolution (45 mm). As in the BMJ runs, the location of precipitation maxima agreed rather well with observations, particularly in the higher-resolution runs. The KF runs accurately depicted the southern Texas maximum, with hints of enhancements near Austin (AUS; see Fig. 8 for location) in central Texas and westward toward Del Rio.

Total domain precipitation (Table 6) increased most rapidly as resolution changed from 78 to 22 km. The changes were comparable to those in the June case, but less than the July case. Of note, total domain precipitation then remained relatively constant as resolution improved more to 12 km.

In the May case, the KF results appeared to behave opposite to the other two events. In other words, instead of the KF scheme playing a minor role in regions of maximum precipitation, resulting in large resolution–

TABLE 6. Domain-integrated total precipitation (10^{12} kg) for the Eta simulations for 27–28 May 1997 using the KF scheme.

Time (h)	78 km	39 km	22 km	12 km
12	5.1	5.5	6.2	5.7
18	6.1	7.3	8.6	8.5

QPF dependence, the KF scheme dominated the production of precipitation, reducing the impact of horizontal resolution changes. Even at 12-km resolution, over 50% of the peak precipitation was produced by the KF scheme. In this case, the inconsistent behavior seems to be explained by the quick activation of the scheme. The exceptionally strong low-level convergence and resulting upward motion, along with unusually high values of low-level moisture, and CAPE, allowed the scheme to trigger during the morning hours, nearly everywhere along the front in Texas. Instability was released before a more concentrated region of heavy precipitation could form. Also of note, the KF simulations did not result in a noticeable boundary propagating southwestward toward Waco during the morning. The convection that developed in the first few hours of the simulation was located farther northwest than in the BMJ simulations (near Paris, TX; PRX in Fig. 8) along the front, and enhanced convergence related to this convection was quickly lost after a few hours of southward propagation, as convection developed all along the front.

5. Discussion and conclusions

The three cases described above evidence strikingly different QPF behavior as horizontal resolution is increased. In addition, the QPF trends differ markedly for different convective parameterizations, even for the same case. Simulations of the June 1996 Iowa flood event using the BMJ scheme show that improved horizontal resolution may have little impact on the peak precipitation simulated in a model. In regions where the convective scheme produces most of the precipitation, and the moisture supply and low-level convergence are of sufficiently large scale, the improved resolution does not increase the QPF significantly. In regions of small-scale forcing, the improved resolution may not overcome other model deficiencies, such as inadequate simulation of low-level instability or convectively produced boundaries. However, reasonable simulation of such features may allow dramatic changes in the QPF to occur at high resolution, as occurred in the 22- and 12-km KF runs.

The July 1996 MCS flash flood event demonstrates significant variations in the impact of horizontal resolution refinements for different convective parameterizations. As in the June case, these variations are due in part to the impact that the convective parameterizations have on the grid-scale thermodynamic parameters. Simulations using the BMJ scheme (currently operational at NCEP) actually show a *decrease* in peak simulated rainfall as resolution improves. Nearly all of the precipitation in this case is generated by the convective scheme. Simulations with the KF scheme, however, are strongly sensitive to horizontal resolution, with much greater precipitation totals occurring at high resolutions. Most of the precipitation in the regions of greatest amount is grid resolved. Significant differences occur in the location of simulated rainfall between runs using the BMJ and KF parameterizations. As further evidence of the difficulties facing forecasters presented with simulations such as these, the BMJ runs, which somewhat accurately indicate the location of heaviest precipitation, seriously underforecast the amounts, even at l2-km resolution, while the KF runs, more accurately simulating excessive rainfall, displace the maximum by several hundred kilometers. The unusual behavior of the schemes for this event appears to be due to other errors in the simulated weather prior to the nocturnal MCS.

The May 1997 convective event again demonstrates large differences in the behavior of the precipitation fields depending on the convective parameterization used. Runs with the BMJ scheme evidence great variation in peak QPF as horizontal resolution varies. This case does include strong low-level convergence that favors significant grid-scale precipitation along with activation of the convective parameterization. Extreme instability present in this case results in gridpoint-like storms whose intensity increases greatly with increasing horizontal resolution. Runs with the KF scheme, however, are relatively insensitive to resolution changes from 78 to 12 km, as the strong mesoscale lift along boundaries causes the scheme to activate too quickly, adversely affecting the simulated evolution of afternoon events.

In both the July 1996 and May 1997 cases, where significant simulated rainfall occurs in close proximity to observed extreme convective rainfalls, the simulated convective portion of the rainfall appears to reach an upper limit. In some cases, this results in an underestimate of the total rainfall. In other cases, it results in the formation of gridpoint-like storms, where simulated rainfall does approach or even exceed observed maximum values. The variability in the results for the three cases supports the findings of Zhang et al. (1994) and Hong and Pan (1998) that the interaction between the subgrid-scale and grid-resolvable precipitation plays a crucial role in the resulting simulation of precipitation.

The simulation of these three flash flood-producing systems has raised several questions with regard to the future of excessive rainfall forecasting.

- If there is no consistent relationship between peak modeled rainfall and horizontal resolution, how can model guidance be best applied to specific events?
- What constitutes a better model forecast, accurate location of the precipitation maximum or accurate simulation of peak amount?
- Can knowledge of the triggering mechanism used by different convective parameterizations help in isolating the best forecast among models using different schemes for a given meteorological scenario?

The large variability in the simulations of these events should raise concerns about the value of relying upon one computationally expensive simulation for forecasting guidance. An alternative to this traditional approach in operational forecasting is to run several computationally inexpensive simulations as an ensemble (e.g., Murphy 1988). Efforts are currently under way to explore the usefulness of short-range ensembles, which may be especially useful for highly variable parameters like precipitation (Du et al. 1997).

Acknowledgments. The author would like to thank Prof. George Kallos and his group at the University of Athens, Greece, for providing the workstation Eta Model and for assistance in its implementation at Iowa State. Additional thanks are given to Drs. Eric Rogers and Tom Black, and Mike Baldwin at NCEP for providing a few fields necessary for running the model. The work benefited greatly from discussions with Dr. Jack Kain. The constructive comments of Dr. Robert Maddox and an anonymous reviewer were appreciated. This work was sponsored by the National Science Foundation/National Oceanic and Atmospheric Administration Grant ATM-9612388 in the USWRP program.

REFERENCES

Betts, A. K., 1986: A new convective adjustment scheme. Part I: Observational and theoretical basis. *Quart. J. Roy. Meteor. Soc.,* **112,** 677–692.

——, and M. J. Miller, 1986: A new convective adjustment scheme. Part II: Single column tests using GATE wave, BOMEX, and arctic air-mass data sets. *Quart. J. Roy. Meteor. Soc.,* **112,** 693–709.

Black, T. M., 1994: The new NMC mesoscale Eta model: Description and forecast examples. *Wea. Forecasting,* **9,** 265–278.

Chen, F., K. Mitchell, J. Schaake, Y. Xue, H.-L. Pan, V. Koren, Q. Y. Duan, M. Ek, and A. Betts, 1996: Modeling of land surface evaporation by four schemes and comparison with FIFE observations. *J. Geophys. Res.,* **101,** 7251–7277.

Corfidi, S. F., 1998: Some thoughts on the role of mesoscale features played in the 27 May 1997 central Texas tornado outbreak. Preprints, *19th Conf. on Severe Local Storms,* Minneapolis, MN, Amer. Meteor. Soc., 177–180.

——, J. H. Merritt, and J. M. Fritsch, 1996: Predicting the movement of mesoscale convective complexes. *Wea. Forecasting,* **11,** 41–46.

Doswell, C. A., III, H. E. Brooks, and R. A. Maddox, 1996: Flash flood forecasting: An ingredients-based methodology. *Wea. Forecasting,* **11,** 560–581.

Du, J., S. L. Mullen, and F. Sanders, 1997: Short-range ensemble forecasting of quantitative precipitation. *Mon. Wea. Rev.,* **125,** 2427–2459.

Gallus, W. A., Jr., and J. F. Bresch, 1997: An intense small-scale wintertime vortex in the midwest United States. *Mon. Wea. Rev.,* **125,** 2787–2807.

Grell, G. A., 1993: Prognostic evaluation of assumptions used by cumulus parameterizations. *Mon. Wea. Rev.,* **121,** 764–787.

Hamill, T. M., and S. J. Colucci, 1998: Evaluation of Eta–RSM ensemble probabilistic precipitation forecasts. *Mon. Wea. Rev.,* **126,** 711–724.

Hong, S.-Y., and H.-L. Pan, 1998: Convective trigger function for a mass-flux cumulus parameterization scheme. *Mon. Wea. Rev.,* **126,** 2599–2620.

Hoxit, L. R., and Coauthors, 1978: Meteorological analysis of the Johnstown, Pennsylvania flash flood, 19–20 July 1977. NOAA Tech. Rep. ERL 401-APCL 43, 71 pp. [NTIS PB-297412.]

Janjic, Z. I., 1994: The step-mountain eta coordinate model: Further developments of the convection, viscous sublayer, and turbulence closure schemes. *Mon. Wea. Rev.,* **122,** 928–945.

Junker, N. W., and J. E. Hoke, 1990: An examination of Nested Grid Model precipitation forecasts in the presence of moderate-to-strong low-level southerly inflow. *Wea. Forecasting,* **5,** 333–344.

Kain, J. S., and J. M. Fritsch, 1992: The role of the convective ''trigger function'' in numerical forecasts of mesoscale convective systems. *Meteor. Atmos. Phys.,* **49,** 93–106.

——, and ——, 1993: Convective parameterization for mesoscale models: The Kain–Fritsch scheme. *The Representation of Cumulus Convection in Numerical Models, Meteor. Monogr.,* No. 46, Amer. Meteor. Soc., 165–170.

Maddox, R. A., L. R. Hoxit, C. F. Chappell, and F. Caracena, 1978: Comparison of meteorological aspects of the Big Thompson and Rapid City flash floods. *Mon. Wea. Rev.,* **106,** 375–389.

——, C. F. Chappell, and L. R. Hoxit, 1979: Synoptic and meso-α aspects of flash flood events. *Bull. Amer. Meteor. Soc.,* **60,** 115–123.

Markowski, P. M., E. N. Rasmussen, J. M. Straka, and D. C. Dowell, 1998a: Observations of low-level baroclinicity generated by anvil shadows. *Mon. Wea. Rev.,* **126,** 2959–2971.

——, J. M. Straka, E. N. Rasmussen, and D. O. Blanchard, 1998b: Variability of helicity during VORTEX. *Mon. Wea. Rev.,* **126,** 2942–2958.

Mesinger, F., 1998: Comparison of quantitative precipitation forecasts by the 48- and by the 29-km Eta model: An update and possible implications. Preprints, *12th Conf. on Numerical Weather Prediction,* Phoenix, AZ, Amer. Meteor. Soc., J22–J23.

——, Z. I. Janjic, S. Nickovic, D. Gavrilov, and D. G. Deaven, 1988: The step mountain coordinate: Model description and performance for cases of alpine cyclogenesis and for a case of an Appalachian redevelopment. *Mon. Wea. Rev.,* **116,** 1493–1518.

Miller, R. C., 1972: Note on Analysis and Severe Storm Forecasting Procedures of the Air Force Global Weather Central. Tech. Rep. 200 (Rev. 1975), Air Weather Service, U.S. Air Force, 190 pp. [Available from Air Weather Service, Scott Air Force Base, IL 62225.]

Molinari, J., and M. Dudek, 1986: Implicit versus explicit convective heating in numerical weather prediction models. *Mon. Wea. Rev.,* **114,** 1822–1831.

——, and ——, 1992: Parameterization of convective precipitation in mesoscale numerical models: A critical review. *Mon. Wea. Rev.,* **120,** 326–344.

Murphy, J. M., 1988: The impact of ensemble forecasts on predictability. *Quart. J. Roy. Meteor. Soc.,* **114,** 463–494.

Nicolini, M., K. M. Waldron, and J. Paegle, 1993: Diurnal oscillations of low-level jets, vertical motion and precipitation: A model case study. *Mon. Wea. Rev.,* **121,** 2588–2610.

Rogers, E., and Coauthors, 1998: Changes to the NCEP Operational ''Early'' Eta Analysis/Forecast System. NWS Tech. Procedures Bull. 447, National Oceanic and Atmospheric Administration/National Weather Service, 14 pp. [Available from National Weather Service, Office of Meteorology, 1325 East–West Highway, Silver Spring, MD 20910.]

Rogers, R. F., and J. M. Fritsch, 1996: A general framework for convective trigger functions. *Mon. Wea. Rev.,* **124,** 2438–2452.

Romero, R., C. Ramis, S. Alonso, C. A. Doswell III, and D. Stensrud, 1998: Mesoscale model simulations of three heavy precipitation events in the western Mediterranean region. *Mon. Wea. Rev.,* **126,** 1859–1881.

Schneider, R. S., N. W. Junker, M. T. Eckert, and T. M. Considine, 1996: The performance of the 29 km Meso Eta model in support of forecasting at the Hydrometeorological Prediction Center. Preprints, *11th Conf. on Numerical Weather Prediction,* Norfolk, VA, Amer. Meteor. Soc., J111–J114.

Senesi, S., P. Bougeault, J.-L. Cheze, P. Cosentino, and R.-M. Thepenier, 1996: The Vaison-la-Romaine flash flood: Mesoscale analysis and predictability issues. *Wea. Forecasting,* **11,** 417–442.

Stensrud, D. J., and J. M. Fritsch, 1994a: Mesoscale convective systems in weakly forced large-scale environments. Part II: Generation of a mesoscale initial condition. *Mon. Wea. Rev.,* **122,** 2068–2083.

——, and ——, 1994b: Mesoscale convective systems in weakly forced large-scale environments. Part III: Numerical simulations and implications for operational forecasting. *Mon. Wea. Rev.,* **122,** 2084–2104.

Vaidya, S. S., and S. S. Singh, 1997: Thermodynamic adjustment parameters in the Betts–Miller scheme of convection. *Wea. Forecasting,* **12,** 819–825.

Weisman, M. L., W. C. Skamarock, and J. B. Klemp, 1997: The resolution dependence of explicitly modeled convective systems. *Mon. Wea. Rev.,* **125,** 527–548.

Zhang, D.-L., and J. M. Fritsch, 1988: Numerical sensitivity experiments of varying model physics on the structure, evolution, and dynamics of two mesoscale convective systems. *J. Atmos. Sci.,* **45,** 261–293.

——, J. S. Kain, J. M. Fritsch, and K. Gao, 1994: Comments on ''Parameterization of convective precipitation in mesoscale numerical models. A critical review.'' *Mon. Wea. Rev.,* **122,** 2222–2231.